Volatility Uncertainty, Disasters, and the Puzzle of VIX Futures Contango

Abstract

The VIX futures curve is most often in contango but displays backwardation during unfavorable market conditions. We construct an explanation based on the notion of stochastic orders of volatility uncertainty — meaning that investors view short-dated volatility uncertainty as *less likely to take on larger values* than long-dated volatility uncertainty — under all pricing measures. We complement this theory of volatility uncertainty with tractable equity price processes whose paths consist of continuous shocks interspersed with jump discontinuities, the latter reflecting disaster uncertainty with time-varying disaster probability.

Keywords: Volatility uncertainty, stochastic orders, disasters, weeklys, hedging instruments, contango

1 Introduction

The VIX futures curve is depicted by connecting prices of futures contracts with different expiration dates. Much like the interest-rate yield curve, it is displayed on a graph where the X-axis represents expiration dates, and the Y-axis represents the VIX futures prices. The underlier is the VIX index created by the Chicago Board Options Exchange (CBOE) and is compiled from traded S&P 500 index option prices. The VIX is itself *not directly traded*. It is gauged by the risk-neutral expectation of a convex function of price fluctuations in the S&P 500 index over the succeeding 30 days.

More often than not, the VIX futures curve consists of the nearest maturity contract having the lowest price and each farther dated contract having a higher price than the previous contract. In other words, the VIX futures curve is typically in contango, that is, upward sloping. This means that long VIX futures positions suffer from roll cost and shorts collect positive carry.

The shape of the VIX futures curve, and its movements through time, is puzzling to practitioners and intensely debated in blog conversations and financial opinion pieces.

As such, two questions are at the core of this paper: What could be the economic rationale for the VIX futures curve being mostly in contango? What could be a justification for the curve to invert to backwardation? To our knowledge, there is no widely accepted economic explanation in the academic journals, and we are not aware of a lead consensus among practitioners.

Salient facts. We illustrate a feature of the equity volatility markets, pertinent to the developed theory, in the following table on VIX futures prices for the six nearest contracts.

Date	T_1	T_2	T_3	T_4	T_5	T_6
11/06/2017	10.8	12.2	13.4	14.1	14.7	15.3
10/16/2008	63.9	42.8	35.5	34.7	34.3	32.7

While the VIX futures curve is in contango on 11/06/2017, the VIX futures curve is in backwardation during the financial crisis (10/16/2008). The interpretation of the inversion is that (i) investors are preoccupied with disaster-type equity and volatility uncertainties and (ii) investors anticipate continued commotion in equity and volatility markets.

In line with the theoretical treatment, our empirical analysis shows that, the VIX futures curve has been in contango on 82% of the days since inception (our sample is 04/25/2006 to 12/31/2019).

Further analysis indicates that the futures curve on the VSTOXX — the volatility index on STOXX 50 equity index — is in contango for 76% of the days between 10/22/2010 and 09/23/2021.

Theoretical explanation. In order to help decipher the sufficient conditions for when the VIX futures curve will be in contango, we exploit the notion of volatility uncertainty being "*stochastically smaller*" in the near term versus the longer term, for *all* pricing measures. Suppose one uses the random variable $\widetilde{Z}_{T_n}$ (for $n = 1, 2, \ldots$) to reflect the valuation at date T_n of volatility uncertainty over $[T_n, T_n + \hbar]$, for contract parameter $\hbar$=30 days. Then, the notion of stochastically smaller, from the standpoint of current date $t < T_1$, refers to the situation in which the probability of $\widetilde{Z}_{T_1}$ exceeding a threshold value $\mathbb{z}$, is *lower* than or equal to the probability of $\widetilde{Z}_{T_2}$ exceeding the same threshold $\mathbb{z}$, and this disparity is true for all $\mathbb{z}$ (under all pricing measures).

Although the notion that short-dated volatility uncertainty is *less likely* to take (relatively) larger values is admittedly abstract, we show its promise in describing the intertemporal realities embedded in the VIX futures curve. We examine the implications of this model-detached approach to order volatility uncertainty when these restrictions are framed in the context of workhorse models. In one of our models, discontinuities in volatility can be correlated with disaster-type price jumps.[1]

Motivated by our empirical depictions, we combine our approach with a model in which the equity price process has both diffusive volatility risks and jump risks (reflecting a disaster component). These equity dynamics encapsulate variability in the probability of disasters. The model reveals that the VIX futures curve is in contango when market participants perceive disaster risks and volatility risks to be *not* pronounced relative to their respective long-run mean level.

In essence, we consider a mechanism by which the workings of the theoretical restrictions align with near-term volatility uncertainty being ordered as stochastically smaller. If the VIX were to increase in response to economic anxieties, it would rearrange the stochastic ordering of volatility uncertainty and, accordingly, the VIX futures curve may slide into backwardation.

Aiming for realism in our theoretical explanation of the VIX futures curve, we adhere to how the payoff underlying the VIX is formulated by the CBOE. Given that the S&P 500 option portfolios that determine the VIX settlement values are not preannounced by the CBOE, it is not possible to explain the VIX futures curve using storage or carry arguments.

[1] Volatility jumps can be economically relevant: High VIX values are associated with backwardation in VIX futures curves, and realizations of unfavorable economic states are connected with volatility jumps to the upside.

2 Volatility data and theory-relevant facts

The understanding of equity index volatility has been widened by studies using the VIX volatility index.[2] In this paper, we answer two questions about movements in the VIX futures curve. First, what could be the channels that reconcile the VIX futures curve being predominantly in contango? Second, why does a pattern of backwardation emerge during periods of market distress?

Our theoretical analysis is motivated by the empirical evidence on intertemporal futures price relations. Hence, first, we present the empirical facts.

Fact 1. VIX futures are in contango in (approximately) 82% of the entries in our daily sample. We exploit daily price observations on VIX futures from consecutive maturities, over the sample period of 04/25/2006 to 12/31/2019. Our data, which is obtained from the CBOE, contains the settlement prices of VIX futures. The start date (04/25/2006) coincides with daily futures prices being available for at least six maturities.[3]

Our depictions exploit a panel of futures prices across 3,447 daily observations. Table 1 reports the essential aspects of the VIX futures curve, combining information from the six nearest-maturity contracts. We denote the futures price at time t for the n-th futures contract by $F_t^{(n)}$.

We extract information on the slope of the futures curves measured across maturities as follows:

$$\text{Slope}_t^{(n)} \;=\; \log(\frac{F_t^{(n)}}{F_t^{(1)}}), \qquad \text{for } n = 2, \ldots, 6. \tag{1}$$

The average $\log(\frac{F_t^{(2)}}{F_t^{(1)}})$ is 5.2% and $\mathbb{1}_{\{\text{Slope}_t^{(2)}>0\}}$ — which represents the fraction of observations with $\log(\frac{F_t^{(2)}}{F_t^{(1)}}) > 0$ — is 81.2%. This baseline finding holds along other points of the futures curve. For example, the average value of $\log(\frac{F_t^{(6)}}{F_t^{(1)}})$ is 13.6%, and it is positive on 82% of days. Our evidence can be interpreted to imply that VIX futures are in backwardation only occasionally.

[2]These contributions include, among others, Grünbichler and Longstaff (1996), Carr and Wu (2006), Duan and Yeh (2007), Carr and Lee (2008), Broadie and Jain (2008), Zhu and Zhang (2007), Zhu and Lian (2011), Lin and Chang (2010), Cont and Kokholm (2013), Mencia and Sentana (2013), Bakshi, Madan, and Panayotov (2015), Park (2016), Eraker and Wu (2017), Johnson (2017), Bardgett, Gourier, and Leippold (2019), Cheng (2019), Eraker and Yang (2020), Hu and Jacobs (2020), and Huang, Schlag, Shaliastovich, and Thimme (2020).

[3]The daily open interest and volume in nearby VIX futures contracts is fairly high. This evidence is presented in Internet Appendix (Table I.1). Volatility uncertainty is actively traded in many forms (Mixon and Onur (2018)).

The tapering of the VIX futures curve can be inferred from the entries in Table 1 (Panel A). This is because the average value of $\log(\frac{F_t^{(6)}}{F_t^{(5)}})$ is 1.4%, as opposed to the average $\log(\frac{F_t^{(2)}}{F_t^{(1)}})$ of 5.2%.

Table 1 (Panel B) reinforces the contango feature based on the following daily regression, pooling data on VIX futures prices across consecutive maturities:

$$\log(F_t^{(n)}) \;=\; \alpha_t \;+\; \beta_t \log(\mathcal{T}_t^{(n)}) \;+\; \epsilon_t^{(n)}, \qquad \text{for } n = 1, \ldots, 6, \text{ and } t = 1, \ldots, \mathbb{T}, \tag{2}$$

where $\mathcal{T}_t^{(n)}$ denotes the remaining term-to-maturity (in days) corresponding to futures contract n. The takeaway is that the hypothesis of the VIX futures curve being flat (i.e., $\beta_t = 0$) is rejected.

Fact 2. The VIX futures curve exhibits backwardation during stressful market states. Table 2 examines the daily slope of the VIX futures curve in conjunction with daily data for the VIX index (Panel A) and for S&P 500 equity index returns (Panel B).

When the VIX is below 18, it is rare for the VIX futures curve not to be in contango. In contrast, the likelihood of backwardation when the VIX is 30 or more is substantially higher. The upshot is that the slope of the VIX futures curve, in particular, whether upward or downward sloping, varies with the VIX. This documented variation in the sign of the slope of the VIX futures curve poses a challenge on theory to reconcile and bears on the design of volatility models.

Using daily S&P 500 equity index returns to represent the market state produces a likewise coherent picture. That is, the shift from contango to backwardation is a phenomenon tied to the realization of unfavorable economic states.

The noteworthy angle from daily S&P 500 index returns is that the VIX futures curve exhibits backwardation when there are large movements of the S&P 500 index to both the downside and the upside. First, the mean slopes are negative when S&P 500 daily returns are less than -3.5% or greater than 3.5%. Second, $\mathbb{1}_{\{\text{Slope}_t^{(n)}>0\}}$ is less than 13%, implying that these market states are predisposed toward backwardation of the VIX futures curve.

The contango feature of volatility futures is preserved for the European VSTOXX volatility index over 10/22/2010 to 09/23/2021. This evidence is shown in Internet Appendix (Tables I.2 and I.3).

Fact 3. Changes in the slope of the VIX futures curve do not move in tandem with changes in the slope of the volatility curve for at-the-money (ATM) S&P 500 index options. This exercise is motivated by the consistent pricing of VIX products and options on the S&P 500 equity index. Our focus on ATM options arises from the known correspondence between equity volatility and ATM equity option prices (e.g., Brenner and Subrahmanyam (1988)).

We build the following time-series of *daily* changes, for $n = 2$ and $n = 4$:

$$\Delta\text{Slope}^{(n)}_{t,\text{spx options}} \equiv \log(\frac{\text{IV}^{(n)}_{t,\text{spx}}}{\text{IV}^{(1)}_{t,\text{spx}}}) - \log(\frac{\text{IV}^{(n)}_{t-1,\text{spx}}}{\text{IV}^{(1)}_{t-1,\text{spx}}}) \qquad \text{and} \tag{3}$$

$$\Delta\text{Slope}^{(n)}_{t,\text{vix futures}} \equiv \log(\frac{F^{(n)}_{t}}{F^{(1)}_{t}}) - \log(\frac{F^{(n)}_{t-1}}{F^{(1)}_{t-1}}), \tag{4}$$

where $\text{IV}^{(n)}_{t,\text{spx}}$ is the average of the implied volatility of ATM puts and calls on the S&P 500 index.

Table 3 reports the joint frequencies of the sign of $\Delta\text{Slope}^{(n)}_{t,\text{vix futures}}$ and $\Delta\text{Slope}^{(n)}_{t,\text{spx options}}$. The sign of $\Delta\text{Slope}^{(n)}_{t,\text{vix futures}}$ is not the same as that of $\Delta\text{Slope}^{(n)}_{t,\text{spx options}}$ for about 36% of the days. Our findings suggest that there may be variables that exert influence on the slope of the VIX futures curves, apart from those that affect the slope of the ATM volatility curves.

Fact 4. Daily VIX time-series is mean-reverting with a Hurst exponent of 0.37. Such a data attribute bears on our theory and on intertemporal assessments of volatility uncertainty.

We use the modified rescaled range analysis of Lo (1991) (and Lo and MacKinlay (2011, Chapter 6.3.1)) to measure long-range dependence in the VIX. Letting $X_j \equiv \log(\frac{\text{VIX}_j}{\text{VIX}_{j-1}})$ denote the daily log change, we consider the expanding windows $\{1 \to \ell\}$ and construct the following:

$$R/S_{\{1\to\ell\}} \equiv \frac{1}{\hat{\sigma}_\ell[q]}(\max_{1\le k\le \ell}\sum_{j=1}^{k}\{X_j - \overline{X}_\ell\} \; - \; \min_{1\le k\le \ell}\sum_{j=1}^{k}\{X_j - \overline{X}_\ell\}), \tag{5}$$

where $\overline{X}_\ell = \frac{1}{\ell}\sum_j X_j$ and $\hat{\sigma}^2_\ell[q] = \hat{\sigma}^2_{\text{x}} + 2\sum_{j=1}^{q}(1 - \frac{j}{q+1})\,\hat{\gamma}_j$ (reflecting devolatilization). The optimal lag q is automatically selected and $\hat{\sigma}^2_{\text{x}}$ and $\hat{\gamma}_j$ are the estimates of variance and autocovariance.

Using an OLS regression, we estimate the model $\log(R/S_{\{1\to\ell\}}) = \text{constant} + \mathbb{H}\log(\ell) + \epsilon_\ell$. The concept of an anti-persistence series maps to an estimate of the Hurst exponent $\mathbb{H}$ between 0 and 0.5. We note that $\mathbb{H}$ is the power law exponent in $R/S_{\{1\to\ell\}} = e^{\text{constant}} \times \ell^{\mathbb{H}}$.

Our estimate of $\mathbb{H}$ of 0.37 (standard error = 0.015) indicates that any downward or upward trend in the VIX will eventually be restored to its long-run parity level. In other words, VIX is mean-reverting and behaves as a bounded random variable.

Fact 5. Two factors describe 99.78% of the cross-sectional variation in daily VIX futures prices. Principal component analysis implies that the first (respectively, second) principal component explains 97.42% (respectively, 2.36%) of the common variation in VIX futures prices.[4]

Each of the futures contracts loads equally and positively on the first principal component. Hence, the first principal component is akin to an *average factor*. In contrast, shorter (respectively, longer) maturity futures contracts load positively (respectively, negatively) on the second principal component. Therefore, the second principal component can be interpreted as (minus of) the slope factor. Fact 5 motivates our consideration of a two-factor driver of the VIX futures curve.

Fact 6. Shorting the VIX futures contract with the most pronounced contango collects the most positive carry. The last column of Table 4 presents the excess return of a dynamically implemented carry strategy that shorts (goes long) the VIX futures contract that exhibits the most (least) pronounced contango. Specifically, each week t (instead of each day), we rank the available VIX futures contracts in ascending order by value of $\frac{F_t^{(n)}}{F_t^{(n-1)}}$, for $n = 1, \ldots, 6$.

For each of the contracts so binned, we first compute the return (summarized in the first six columns of Table 4) of the fully collateralized (long) futures position over the subsequent week. The positions are dynamically rebalanced for each of 743 weeks (5/23/2006 to 8/11/2020).

In the construction of the carry, we assign 1/2 dollar to the long and the short legs. The average weekly (respectively, annualized) return to the carry strategy is 0.44% (respectively, 22.88%) with a standard deviation of 3.10% (respectively, 22.35%). The 95% bootstrap confidence intervals for the average carry returns do not bracket zero and are statistically significant. The carry strategy yields an annualized Sharpe ratio of 1.013.

Our description of the empirical data provides the anchoring groundwork to map the contango and backwardation of the VIX (and VSTOXX) futures curve to a theoretical framework.

[4]This analysis is presented in the Internet Appendix (Table I.4).

3 A theory of VIX futures contango and backwardation

The VIX is not directly traded or storable for delivery. This section formulates a problem to depict the slope of the VIX futures curve, subject to the correct pricing of claims on the VIX and claims on the S&P 500 equity index. Our solution to the problem hinges on the properties of random variables, at two different dates, being "stochastically smaller or larger." Then, we employ this notion of "stochastically smaller or larger" in conjunction with models of equity index prices.

The substance of the model analysis is to associate the state of the VIX futures curve to intertemporal perceptions about the probability of disasters and return volatility. Our point of departure is the link of time-varying disaster probabilities to the VIX futures curve and subsequent volatility uncertainty.

3.1 Uncovering the restrictions of VIX futures contango and backwardation

In what follows, let $(\Omega, \mathcal{I}, (\mathcal{I}_t)_{0\leq t\leq \mathcal{T}}, \mathbb{P})$ be a filtered probability space, with $\mathcal{T}$ being a fixed, finite time. The filtration $(\mathcal{I}_t)_{0\leq t\leq \mathcal{T}}$ satisfies the usual conditions. All stochastic processes with a subscript t are $\mathcal{I}_t$-measurable. The processes are assumed to be right continuous with left limits.

Here, $\mathbb{P}$ denotes the physical probability measure. We denote the equivalent martingale (pricing) measure consistent with no-arbitrage and the pricing kernel M_t by $\mathbb{Q}$. Since markets are not complete, $\mathbb{Q}$ is not unique. Fixing notation, $\mathbb{E}^{\mathbb{Q}}(\bullet|\mathcal{I}_t)$ is the expectation under $\mathbb{Q}$, *conditional* on $\mathcal{I}_t$.

We denote by S_t the price, at time t, of the S&P 500 equity market index. Hereon, we assume that S_t is a *semimartingale*. Let the interest rate be r, a constant.

Furthermore, we denote by $H_t^{t+\hbar}$ the price, at time t, of the S&P 500 futures contract, with maturity at $t+\hbar$. Then, by the cost of carry relation, $H_t^{t+\hbar} = e^{r\,\hbar}\, S_t$.

Problem 1 (Value of VIX_t) *Determine, as per the CBOE (2006) white paper,*

$$\mathrm{VIX}_t \;\equiv\; \sqrt{\mathbb{E}^{\mathbb{Q}}\left(\{-\frac{2}{\hbar}\}\,\log(\frac{S_{t+\hbar}}{H_t^{t+\hbar}})\Big|\mathcal{I}_t\right)}, \qquad \text{with} \qquad \hbar \equiv \frac{30}{365}. \tag{6}$$

The random variable $\{-\frac{2}{\hbar}\}\log(\frac{S_{t+\hbar}}{H_t^{t+\hbar}})$ is convex in $S_{t+\hbar}$, and it has nonnegative expectation. □

The CBOE circumvented Problem 1's reliance on the exact nature of $\mathcal{I}_t$ and a model for $S_{t+\hbar}$ by approximating VIX_t^2 through a portfolio of traded index put and call options.[5]

Denote the nonnegative random variables, representing volatility uncertainty, pertaining to maturity dates $T_1 < T_2$, as follows (we suppress the dependence of $\widetilde{Z}_{T_n}$ on $\hbar$):

$$\widetilde{Z}_{T_1} \;\equiv\; \mathbb{E}^{\mathbb{Q}}(\{-\frac{2}{\hbar}\}\log(\frac{S_{T_1+\hbar}}{H_{T_1}^{T_1+\hbar}})\Big|\mathcal{I}_{T_1}) \qquad \text{and} \qquad \widetilde{Z}_{T_2} \;\equiv\; \mathbb{E}^{\mathbb{Q}}(\{-\frac{2}{\hbar}\}\log(\frac{S_{T_2+\hbar}}{H_{T_2}^{T_2+\hbar}})\Big|\mathcal{I}_{T_2}). \tag{7}$$

We denote by F_t^T the VIX futures price, at time t, with expiration at T. Since F_t^T is a martingale under $\mathbb{Q}$, we have $F_t^T = \mathbb{E}^{\mathbb{Q}}(F_\ell^T\big|\mathcal{I}_t)$, for all t and ℓ satisfying $t \le \ell \le T$.

Problem 2 (VIX futures curve) *The problem entails establishing restrictions under which*

$$F_t^{T_1} \text{ is less than, or greater than, } F_t^{T_2} \text{ for VIX futures maturities } T_1 < T_2, \tag{8}$$

$$\text{where} \quad F_t^T = \mathbb{E}^{\mathbb{Q}}(\text{VIX}_T\Big|\mathcal{I}_t) = \mathbb{E}^{\mathbb{Q}}(\sqrt{\mathbb{E}^{\mathbb{Q}}(\{-\frac{2}{\hbar}\}\log(\frac{S_{T+\hbar}}{H_T^{T+\hbar}})\Big|\mathcal{I}_T)}\;\Big|\mathcal{I}_t). \tag{9}$$

Equation (9) holds because at expiration $F_T^T = \text{VIX}_T$. □

Equation (9) of Problem 2 does *not enable model-free* tractability. The obstacle is that $\widetilde{Z}_{T_n}$ is the time T_n price of yet another subsequent payoff transpiring between T_n and $T_n+\hbar$, for $n = 1, \ldots, N$.

However, a general, as opposed to parametric, property that offers cues to the shape of the VIX futures curve can be constructed based on Ross (1984, Chapter 9.1). We pursue this analysis to ascertain whether, and when, the VIX futures curve may be in contango or backwardation, and we emphasize economic interpretations.

Mindful of our goals, denote the distribution function of $\widetilde{Z}_{T_n}$, under the pricing measure $\mathbb{Q}$, as $\mathbb{G}_{T_n}$. Assume that $\mathbb{E}^{\mathbb{Q}}(\widetilde{Z}_{T_n}\big|\mathcal{I}_t)$ is finite for all $n = 1, \ldots, N$. Suppose

$$\text{Prob}^{\mathbb{Q}}[\widetilde{Z}_{T_1} \ge \mathbb{z}] \;\le\; \text{Prob}^{\mathbb{Q}}[\widetilde{Z}_{T_2} \ge \mathbb{z}], \qquad \text{for all} \;\; \mathbb{z} \in (0, \infty). \tag{10}$$

Then we say that $\widetilde{Z}_{T_1}$ is stochastically *smaller* than $\widetilde{Z}_{T_2}$, written $\widetilde{Z}_{T_1} \le_{\text{st}} \widetilde{Z}_{T_2}$, for $T_1 < T_2$.

[5] Specifically, $\text{VIX}_t^2 \approx \frac{2e^{r\hbar}}{\hbar}(\int_{K<H_t^{t+\hbar}} \frac{\text{put}_t^{\text{spx}}[K;t+\hbar]}{K^2}\,dK + \int_{K>H_t^{t+\hbar}} \frac{\text{call}_t^{\text{spx}}[K;t+\hbar]}{K^2}dK)$ for S&P 500 index options with strike price K and remaining term-to-maturity $\hbar = \frac{30}{365}$. The VIX_t is a widely respected (model-free and forward-looking) measure of return dispersion over the period t to $t+\hbar$.

Result 1 *If* $\widetilde{Z}_{T_1} \leq_{\text{st}} \widetilde{Z}_{T_2}$*, for* $\widetilde{Z}_{T_1}$ *and* $\widetilde{Z}_{T_2}$ *defined in equation (7), then*

$$(a) \qquad \mathbb{E}^{\mathbb{Q}}(\widetilde{Z}_{T_1}\big|\mathcal{I}_t) \;\leq\; \mathbb{E}^{\mathbb{Q}}(\widetilde{Z}_{T_2}\big|\mathcal{I}_t). \tag{11}$$

$$(b) \qquad \underbrace{\mathbb{E}^{\mathbb{Q}}(\sqrt{\widetilde{Z}_{T_1}}\Big|\mathcal{I}_t)}_{\equiv\, F_t^{T_1}} \;\leq\; \underbrace{\mathbb{E}^{\mathbb{Q}}[\sqrt{\widetilde{Z}_{T_2}}\Big|\mathcal{I}_t]}_{\equiv\, F_t^{T_2}}. \tag{12}$$

Proof: See Appendix A. ■

In the setting of Result 1, $\widetilde{Z}_{T_n}$ captures the time T_n price of dispersion expected to prevail over $[T_n, T_n + \hbar]$. In this light, what does it mean economically that $\widetilde{Z}_{T_1}$ is stochastically smaller than $\widetilde{Z}_{T_2}$? The intuition is that the relation $\text{Prob}^{\mathbb{Q}}[\widetilde{Z}_{T_1} \geq \mathbb{z}] \leq \text{Prob}^{\mathbb{Q}}[\widetilde{Z}_{T_2} \geq \mathbb{z}]$ implies that $\widetilde{Z}_{T_1}$ is *less* likely than $\widetilde{Z}_{T_2}$ to take on *larger values*, where the notion of "large" means any value greater than $\mathbb{z}$, and this is true for all values of $\mathbb{z}$.

The implication that $\widetilde{Z}_{T_1} \leq_{\text{st}} \widetilde{Z}_{T_2}$ is consistent with $\mathbb{E}^{\mathbb{Q}}(\widetilde{Z}_{T_1}\big|\mathcal{I}_t) \leq \mathbb{E}^{\mathbb{Q}}(\widetilde{Z}_{T_2}\big|\mathcal{I}_t)$ enables simplifications because $\mathbb{E}^{\mathbb{Q}}(\sqrt{\bullet}\big|\mathcal{I}_t)$ is not analytically tractable, even under model parameterizations. Additionally, our approach, as seen in the sequel, helps to trace the macroeconomic sources that determine the shape of the VIX futures curve.

Shaked and Shantikumar (2006, Chapter 5) introduce the notion of the Laplace transform order, denoted by $\widetilde{Z}_{T_1} \leq_{\text{Lt}} \widetilde{Z}_{T_2}$. If $\mathbb{E}^{\mathbb{Q}}(e^{-u\,\widetilde{Z}_{T_1}}\big|\mathcal{I}_t) \geq \mathbb{E}^{\mathbb{Q}}(e^{-u\,\widetilde{Z}_{T_2}}\big|\mathcal{I}_t)$, for $u \in (0, \infty)$, then they postulate that $\widetilde{Z}_{T_1}$ is smaller than $\widetilde{Z}_{T_2}$ in the Laplace transform order. Importantly, $\widetilde{Z}_{T_1} \leq_{\text{Lt}} \widetilde{Z}_{T_2} \Longrightarrow \mathbb{E}^{\mathbb{Q}}(\widetilde{Z}_{T_1}\big|\mathcal{I}_t) \leq \mathbb{E}^{\mathbb{Q}}(\widetilde{Z}_{T_2}\big|\mathcal{I}_t)$.

Due to a representation by Schürger (2002), one may, thus, express

$$\sqrt{\widetilde{Z}_{T_1}} = \frac{1}{2\sqrt{\pi}} \int_0^\infty \frac{1 - e^{-u\,\widetilde{Z}_{T_1}}}{u^{3/2}} du. \;\text{ Hence, }\; \mathbb{E}^{\mathbb{Q}}(\sqrt{\widetilde{Z}_{T_1}}\big|\mathcal{I}_t) = \frac{1}{2\sqrt{\pi}} \int_0^\infty \frac{1 - \mathbb{E}^{\mathbb{Q}}(e^{-u\,\widetilde{Z}_{T_1}}\big|\mathcal{I}_t)}{u^{3/2}} du. \tag{13}$$

Therefore, the Laplace transform order can potentially be connected to $\mathbb{E}^{\mathbb{Q}}(\sqrt{\widetilde{Z}_{T_1}}\big|\mathcal{I}_t) \leq \mathbb{E}^{\mathbb{Q}}(\sqrt{\widetilde{Z}_{T_2}}\big|\mathcal{I}_t)$.

We focus on the stochastic order $\leq_{\text{st}}$, instead of $\leq_{\text{Lt}}$, as the restriction of $\mathbb{E}^{\mathbb{Q}}(\widetilde{Z}_{T_1}\big|\mathcal{I}_t) \leq \mathbb{E}^{\mathbb{Q}}(\widetilde{Z}_{T_2}\big|\mathcal{I}_t)$ is often tractable to validate, and because it is revealing about the intertemporal formation of beliefs in the market for volatility trading. We investigate whether the VIX contango feature is tied to the mean of $\widetilde{Z}_{T_n}$, while not discarding a role for higher-order moment effects.

3.2 Disaster probability, return volatility, and VIX futures curve

In this section, we consider a plausible stochastic structure with the aim of uncovering clearer analytics. Our featured ingredients of volatility uncertainty $\widetilde{Z}_{T_n}$, for $n = 1, \ldots, N$, are time-varying probability of disasters and stochastic return volatility.

The following features of disaster-type risks and volatility motivate the considered models:

1. *Changes in the slope of the VIX futures curve are predictable.* Predictors constructed from VIX and S&P 500 options (e.g., jump risks and butterfly spreads inferred from VIX options and quadratic variation of the S&P 500 returns) forecast changes in the slope of the VIX futures curve. See the evidence in Table I.5 (Internet Appendix (Section A.1)). These predictors can be viewed as encoding information about disaster risks or return volatility risks.

2. *30-day ATM implied volatilities extracted from S&P 500 index options are more pronounced than their 60-day counterparts (that is, bend downwards) on 46% of the days in our sample.* Furthermore, ATM implied volatilities exhibit time-variation.

3. *Volatility uncertainty $\widetilde{Z}_T$ generically relates to the price of local time (essentially strike dependent volatility) and the price of jumps across the strike.* Internet Appendix (Section A.2) elicits the intuition that, at time t, investors draw an intertemporal distinction between the pricing of local time and the pricing of jumps across the strike. Our model parameterizes these links in a parsimonious way and makes the channels we seek analytically transparent.

Proceeding, the salient aspect of the ensuing model is that it incorporates *time-varying probability of disasters* $\boldsymbol{\lambda}_t$. With $\mathbb{E}^{\mathbb{Q}}(\bullet)$ denoting unconditional expectation, the equity index price dynamics is

$$\text{Size of disasters:} \quad x \qquad \text{follows (unspecified) i.i.d. distribution under } \mathbb{Q} \tag{14}$$

$$\text{Equity index price :} \quad \frac{dS_t}{S_{t-}} = r\,dt + \sqrt{\mathbf{v}_t}\,d\mathbb{B}_t^{\mathbb{Q},\mathrm{s}} + (e^x - 1)\,d\mathbb{N}_t^{\mathbb{Q}} - \boldsymbol{\lambda}_t\,\mathbb{E}^{\mathbb{Q}}(e^x - 1)dt \tag{15}$$

$$\text{Poisson jump :} \quad d\mathbb{N}_t^{\mathbb{Q}} = \begin{cases} 1 & \text{with probability } \boldsymbol{\lambda}_t\,dt \\ 0 & \text{with probability } 1 - \boldsymbol{\lambda}_t\,dt \end{cases} \tag{16}$$

$$\text{Diffusive variance :} \quad d\mathbf{v}_t = (\theta_{\mathrm{vol}} - \kappa_{\mathrm{vol}}\,\mathbf{v}_t)\,dt + \sigma_{\mathrm{vol}}\sqrt{\mathbf{v}_t}\,d\mathbb{B}_t^{\mathbb{Q},\mathbf{v}} \tag{17}$$

$$\text{Disaster probability :} \quad d\boldsymbol{\lambda}_t = (\theta_\lambda - \kappa_\lambda\,\boldsymbol{\lambda}_t)\,dt + \sigma_\lambda\sqrt{\boldsymbol{\lambda}_t}\,d\mathbb{B}_t^{\mathbb{Q},\boldsymbol{\lambda}}. \tag{18}$$

The standard Brownian motion $\mathbb{B}_t^{\mathbb{Q},\mathrm{s}}$ is correlated with $\mathbb{B}_t^{\mathbb{Q},\mathbf{v}}$, whereas the standard Brownian motion $\mathbb{B}_t^{\mathbb{Q},\boldsymbol{\lambda}}$ is uncorrelated with all other sources of risk.[6]

Complementing Result 1, it is seen (see Appendix B) that, for generic futures maturity T,

$$\widetilde{Z}_T = 2 \underbrace{\{\mathbb{E}^{\mathbb{Q}}(e^x - 1 - x)\}}_{\geq 0 \text{ (Jensen's inequality)}} [\frac{\theta_\lambda}{\kappa_\lambda} + \frac{(1-e^{-\kappa_\lambda \hbar})}{\hbar \kappa_\lambda}(\boldsymbol{\lambda}_T - \frac{\theta_\lambda}{\kappa_\lambda})] + \frac{\theta_{\mathrm{vol}}}{\kappa_{\mathrm{vol}}} + \frac{(1-e^{-\kappa_{\mathrm{vol}}\hbar})}{\hbar\,\kappa_{\mathrm{vol}}}(\mathbf{v}_T - \frac{\theta_{\mathrm{vol}}}{\kappa_{\mathrm{vol}}}). \tag{19}$$

In this model, disaster probabilities and return variance are the source of the variation in $\widetilde{Z}_T$. Thus, the futures price $F_t^T = \mathbb{E}^{\mathbb{Q}}(\sqrt{\widetilde{Z}_T}\big|\mathcal{I}_t)$ inherits a two-factor structure (in line with Fact 5).

What, then, are the influences that determine intertemporal futures price relations? If $\widetilde{Z}_{T_1}$ is stochastically smaller than $\widetilde{Z}_{T_2}$, that is, $\widetilde{Z}_{T_1} \leq_{\mathrm{st}} \widetilde{Z}_{T_2}$, then it must hold (using the known analytical form of $\mathbb{E}^{\mathbb{Q}}(\mathbf{v}_T\big|\mathcal{I}_t)$ and $\mathbb{E}^{\mathbb{Q}}(\boldsymbol{\lambda}_T\big|\mathcal{I}_t)$; see Appendix B) that, for $T_1 < T_2$,

$$\begin{aligned} 0 \;\geq\; & \overbrace{\mathbb{E}^{\mathbb{Q}}(\widetilde{Z}_{T_1}\big|\mathcal{I}_t) \;-\; \mathbb{E}^{\mathbb{Q}}(\widetilde{Z}_{T_2}\big|\mathcal{I}_t)}^{\text{from equation (11) of Result 1}} \qquad \text{implying, in turn, by equation (19), that} \\ =\; & 2\{\underbrace{(\mathbb{E}^{\mathbb{Q}}(e^x - 1 - x)}_{\geq 0} \underbrace{\frac{(1-e^{-\kappa_\lambda \hbar})}{\hbar\,\kappa_\lambda}}_{>0}\} \underbrace{\{e^{-\kappa_\lambda(T_1-t)} - e^{-\kappa_\lambda(T_2-t)}\}}_{>0}(\boldsymbol{\lambda}_t - \frac{\theta_\lambda}{\kappa_\lambda}) \\ & + \underbrace{\frac{(1-e^{-\kappa_{\mathrm{vol}}\hbar})}{\hbar\,\kappa_{\mathrm{vol}}}}_{>0} \underbrace{\{e^{-\kappa_{\mathrm{vol}}(T_1-t)} - e^{-\kappa_{\mathrm{vol}}(T_2-t)}\}}_{>0}(\mathbf{v}_t - \frac{\theta_{\mathrm{vol}}}{\kappa_{\mathrm{vol}}}). \end{aligned} \tag{20}$$

Therefore, in light of Result 1 (equation (12)), it holds that, for $\mathbb{E}^{\mathbb{Q}}(\widetilde{Z}_{T_1}\big|\mathcal{I}_t) - \mathbb{E}^{\mathbb{Q}}(\widetilde{Z}_{T_2}\big|\mathcal{I}_t) < 0$,

$$\underbrace{\text{Shape of Futures Curve}_t}_{F_t^{T_2} \;-\; F_t^{T_1}} \;=\; \begin{cases} \text{Contango} & \text{if} \quad \boldsymbol{\lambda}_t < \frac{\theta_\lambda}{\kappa_\lambda} \;\text{ and }\; \mathbf{v}_t < \frac{\theta_{\mathrm{vol}}}{\kappa_{\mathrm{vol}}} \\ \text{Backwardation} & \text{if} \quad \boldsymbol{\lambda}_t > \frac{\theta_\lambda}{\kappa_\lambda} \;\text{ and }\; \mathbf{v}_t > \frac{\theta_{\mathrm{vol}}}{\kappa_{\mathrm{vol}}}. \end{cases} \tag{21}$$

The conceptual implication is that when investors perceive time t volatility or disaster risk to be more pronounced relative to a long-term norm (i.e., the long-run reversion levels $\frac{\theta_{\mathrm{vol}}}{\kappa_{\mathrm{vol}}}$ and $\frac{\theta_\lambda}{\kappa_\lambda}$), then

[6] To develop the implications of Result 1, we draw on the time-varying intensity models considered in Santa-Clara and Yan (2010), Aït-Sahalia and Jacod (2012), Gabaix (2012), Wachter (2013), and Aït-Sahalia, Cacho-Diaz, and Laeven (2015), combined with diffusive volatility. The role of volatility uncertainty is analyzed from alternative perspectives in Andersen, Bollerslev, Diebold, and Labys (2003), Andersen, Bollerslev, and Diebold (2007), Todorov (2010), Drechsler and Yaron (2011), Bates (2012), Dew-Becker, Giglio, Le, and Rodriguez (2017), Amengual and Xiu (2018), Aït-Sahalia, Karaman, and Mancini (2020), Eraker and Yang (2020), Lochstoer and Muir (2020), Aït-Sahalia, Li, and Li (2021), and Ai, Han, and Xu (2021).

shorter-dated VIX futures contracts are more expensive than longer ones and the futures curve is backwardated. This aspect of our formalization is founded in our empirical observations.

If $\boldsymbol{\lambda}_t < \frac{\theta_\lambda}{\kappa_\lambda}$ and $\mathbf{v}_t > \frac{\theta_{\text{vol}}}{\kappa_{\text{vol}}}$ (or the reverse), then the distinction between contango and backwardation is established by prevailing market conditions. In this case, the net quantitative effect can be ascribed to diffusive volatility and disaster probability departing from their respective long-run levels. The support for this view can be gleaned from Table 2 (Panel A), which provides the pattern on contango and backwardation in relation to the realizations of VIX higher than 30.

The theory of uncertainty about disaster probabilities and return volatility is an attempt to reconcile observed VIX futures prices. Our theory sheds light on the effects of economic expectations in the market for volatility trading.

Our model approach tells us that investors may perceive the pricing of volatility and disaster risks to be less open-ended over shorter-dated VIX futures contracts, as opposed to longer-dated contracts. In other words, the projections about the outlook for volatility and disaster risks may become more *uncertain* the further into the future one examines. If adverse economic conditions perturb this projection, then the VIX futures curve can slip to backwardation. Our theory implies that when negative sentiment about equities recedes, the VIX futures curve favors contango.

3.3 Extension: Disaster probability, and jumps in both price and volatility

Consider the following theoretical environment, which modifies the model of Duffie, Pan, and Singleton (2000) to incorporate stochastic intensity. The details are in Appendix C.

$$\text{Equity index price}: \quad \frac{dS_t}{S_{t-}} = r\,dt + \sqrt{\mathbf{v}_t}\,d\mathbb{B}_t^{\mathbb{Q},\text{s}} + (e^{x_s}-1)\,d\mathbb{N}_t^{\mathbb{Q}} - \boldsymbol{\lambda}_t\,\mathbb{E}^{\mathbb{Q}}(e^{x_s}-1)dt \tag{22}$$

$$\text{Joint Poisson jump}: \quad d\mathbb{N}_t^{\mathbb{Q}} = \begin{cases} 1 & \text{with probability } \boldsymbol{\lambda}_t\,dt \\ 0 & \text{with probability } 1-\boldsymbol{\lambda}_t\,dt \end{cases} \tag{23}$$

$$\text{Disaster probability}: \quad d\boldsymbol{\lambda}_t = (\theta_\lambda - \kappa_\lambda\,\boldsymbol{\lambda}_t)\,dt + \sigma_\lambda\sqrt{\boldsymbol{\lambda}_t}\,d\mathbb{B}_t^{\mathbb{Q},\boldsymbol{\lambda}} \tag{24}$$

$$\text{Size of } \textit{additive} \text{ jumps in } \mathbf{v}_t\text{: } x_{\mathbf{v}} \quad \text{follows spectrally positive i.i.d. distribution (under } \mathbb{Q}) \tag{25}$$

$$\text{Size of } \textit{percentage} \text{ disasters: } x_s \quad \text{has an i.i.d. distribution conditional on } x_{\mathbf{v}} \text{ (under } \mathbb{Q}) \tag{26}$$

$$\text{Variance}: \quad d\mathbf{v}_t = (\theta_{\text{vol}} - \kappa_{\text{vol}}\mathbf{v}_t)dt + \sigma_{\text{vol}}\sqrt{\mathbf{v}_t}d\mathbb{B}_t^{\mathbb{Q},\mathbf{v}} + \underbrace{x_{\mathbf{v}}\,d\mathbb{N}_t^{\mathbb{Q}}}_{\text{jumps in } \mathbf{v}_t}. \tag{27}$$

For this model, in which x_s and $x_{\mathbf{v}}$ can be correlated, we derive the following (for $T_1 < T_2$):

$$
\begin{aligned}
0 \;\geq\; & \overbrace{\mathbb{E}^{\mathbb{Q}}(\widetilde{Z}_{T_1}|\mathcal{I}_t) \;-\; \mathbb{E}^{\mathbb{Q}}(\widetilde{Z}_{T_2}|\mathcal{I}_t)}^{\text{from equation (11) of Result 1}} \\
= \;& \underbrace{-\;\frac{\mathbb{E}^{\mathbb{Q}}(x_{\mathbf{v}})(1-e^{-\kappa_{\text{vol}}\,\hbar})}{\hbar\,\kappa_{\text{vol}}}\,\{e^{-\kappa_{\text{vol}}(T_1-t)}-e^{-\kappa_{\text{vol}}(T_2-t)}\}(\frac{\theta_\lambda}{\kappa_\lambda\,\kappa_{\text{vol}}})}_{\equiv\ \text{Term 1} \,<\, 0} \\
& \underbrace{-\;\frac{\mathbb{E}^{\mathbb{Q}}(x_{\mathbf{v}})(1-e^{-\kappa_{\text{vol}}\,\hbar})}{\hbar\,\kappa_{\text{vol}}}\;\frac{[\{e^{-\kappa_{\text{vol}}(T_1-t)}-e^{-\kappa_{\text{vol}}(T_2-t)}\}-\{e^{-\kappa_\lambda(T_1-t)}-e^{-\kappa_\lambda(T_2-t)}\}]}{\kappa_{\text{vol}}-\kappa_\lambda}(\boldsymbol{\lambda}_t-\frac{\theta_\lambda}{\kappa_\lambda})}_{\equiv\ \text{Term 2} \,<\, 0} \\
& \underbrace{+\;\frac{\mathbb{E}^{\mathbb{Q}}(x_{\mathbf{v}})}{\hbar\,\kappa_{\text{vol}}}\,\{\frac{(e^{-\kappa_{\text{vol}}\hbar}-e^{-\kappa_\lambda\hbar})}{(\kappa_{\text{vol}}-\kappa_\lambda)}+\frac{(1-e^{-\kappa_\lambda\hbar})}{\kappa_\lambda}\}\,(e^{-\kappa_\lambda(T_1-t)}-e^{-\kappa_\lambda(T_2-t)})\,(\boldsymbol{\lambda}_t-\frac{\theta_\lambda}{\kappa_\lambda})}_{\equiv\ \text{Term 3} \,>\, 0} \\
& \underbrace{+\,2\,\underbrace{\mathbb{E}^{\mathbb{Q}}(e^{x_s}-1-x_s)}_{\geq 0}\;\frac{(1-e^{-\kappa_\lambda\hbar})}{\hbar\,\kappa_\lambda}\,\underbrace{(e^{-\kappa_\lambda(T_1-t)}-e^{-\kappa_\lambda(T_2-t)})}_{>0}(\boldsymbol{\lambda}_t-\frac{\theta_\lambda}{\kappa_\lambda})}_{\equiv\ \text{Term 4} \,>\, 0} \\
& +\;\underbrace{\frac{(1-e^{-\kappa_{\text{vol}}\,\hbar})}{\hbar\,\kappa_{\text{vol}}}(e^{-\kappa_{\text{vol}}(T_1-t)}-e^{-\kappa_{\text{vol}}(T_2-t)})}_{>\,0}\,(\mathbf{v}_t-\frac{\theta_{\text{vol}}}{\kappa_{\text{vol}}}).
\end{aligned}
\tag{28}
$$

Our quantitative evaluations back a finding that Term 4 (related to the jumps in the equity index price) dominates Term 2 and Term 3 (the terms related to jumps in $\mathbf{v}_t$). The intuition is that disaster-type price jumps exert a stronger effect on the slope of the VIX futures curve.[7]

Thus, the notion of $\widetilde{Z}_{T_1}$ being stochastically smaller than $\widetilde{Z}_{T_2}$ (that is, $\mathbb{E}^{\mathbb{Q}}(\widetilde{Z}_{T_1}|\mathcal{I}_t) \leq \mathbb{E}^{\mathbb{Q}}(\widetilde{Z}_{T_2}|\mathcal{I}_t)$) is preserved when $\boldsymbol{\lambda}_t$ is below $\frac{\theta_\lambda}{\kappa_\lambda}$ and $\mathbf{v}_t$ is below $\frac{\theta_{\text{vol}}}{\kappa_{\text{vol}}}$.[8] These theoretical restrictions align with the VIX futures curve being in contango.

3.4 Examining the empirical implications of the theory using weeklys

If $\boldsymbol{\lambda}_t < \frac{\theta_\lambda}{\kappa_\lambda}$ and $\mathbf{v}_t < \frac{\theta_{\text{vol}}}{\kappa_{\text{vol}}}$, then our theory implies that the VIX futures curve would be in contango. In this section, we examine the confirmatory instances of this theory by constructing a measure of risk-neutral disaster probability from weekly put options (the *weeklys*) on the S&P 500 index.

In Merton (1976), the risk-neutral probability of *one* significant event over an infinitesimal Δt is $\boldsymbol{\lambda}_t\,\Delta t$, while the probability of two or more jumps is negligible. We associate this event to a

[7] The work of Todorov and Tauchen (2011) and Bandi and Reno (2016) implies that both the equity price and its volatility jump (that is, volatility can jump both down and up).

[8] Recognize that Term 1, as defined in equation (28), is negative.

large equity decline — a disaster — over Friday to Friday. Using weeklys on the S&P 500 index, we measure the risk-neutral disaster probability as follows:

$$\begin{aligned} \underbrace{\boldsymbol{\lambda}_t \, \Delta t}_{\substack{\text{Risk-neutral disaster probability} \\ (\Delta t \, = \, 1/52 \text{ (one week)})}} &\approx \mathbb{E}^{\mathbb{Q}}(\mathbb{1}_{\{\frac{S_{t+\Delta t}}{S_t}-1 \, < \, -k_{\text{disaster}}\}} \big| \mathcal{I}_t) \\ &\approx e^{r\Delta t} \times \frac{\text{put}_t[K^{\text{disaster}} + \Delta K] \; - \; \text{put}_t[K^{\text{disaster}} - \Delta K]}{2 \, \Delta \, K}, \end{aligned} \tag{29}$$

for small strike price increment ΔK and $\frac{K^{\text{disaster}}}{S_t} - 1 = -k_{\text{disaster}} < 0$, where $k_{\text{disaster}} = 0.08$ or 0.10. On average, a disaster more severe than 8% (respectively, 10%) maps to a put delta of -0.51% (respectively, -0.27%).

There are 519 weekly cycles in our sample of put options and VIX futures. The first (last) cycle consists of the closing put prices on 1/7/2011 (12/11/2020) for options expiring on 1/14/2011 (12/18/2020). In line with our daily evidence, the VIX futures curve is in contango for 84% of the Fridays. This depiction relies on the front-month and second-month VIX futures contracts.

3.4.1 Empirical hypothesis

To assess the link between the theory (that is, equation (21)) and empirics, we consider an approach for which data can be constructed. Whereas we have utilized, known at time t, put prices to synthesize the probability of an unlikely event, the model-free measurement of $\mathbf{v}_t$ is not feasible (to our knowledge).

Guided by such an implication, we formulate, and empirically investigate, the following hypothesis:

$$\mathbb{1}_{\{\text{slope of the VIX futures curve}_t > 0\}} \; - \; \underbrace{\{\mathbb{1}_{\{\boldsymbol{\lambda}_t < \frac{\theta_\lambda}{\kappa_\lambda}\}} \text{ and } \mathbb{1}_{\{\mathbf{v}_t < \frac{\theta_{\text{vol}}}{\kappa_{\text{vol}}}\}}\}}_{\approx \text{ measured by } \mathbb{1}_{\{\boldsymbol{\lambda}_t < \frac{\theta_\lambda}{\kappa_\lambda}\}}} \; = \; 0. \quad \text{(state-by-state)} \tag{30}$$

In implementation, we proxy the occurrence of $\mathbb{1}_{\{\boldsymbol{\lambda}_t < \frac{\theta_\lambda}{\kappa_\lambda}\}}$ and $\mathbb{1}_{\{\mathbf{v}_t < \frac{\theta_{\text{vol}}}{\kappa_{\text{vol}}}\}}$ by $\mathbb{1}_{\{\boldsymbol{\lambda}_t < \frac{\theta_\lambda}{\kappa_\lambda}\}}$. There would be a mismatch with the theory, if there is a substantial number of instances of the VIX futures contango (respectively, backwardation) deviating from the occurrence of $\boldsymbol{\lambda}_t < \frac{\theta_\lambda}{\kappa_\lambda}$ (respectively,

$\boldsymbol{\lambda}_t > \frac{\theta_\lambda}{\kappa_\lambda}$). That is, the theory would be undermined if short-dated volatility uncertainty is smaller than its long-dated counterpart while the VIX futures curve contradicts by being backwardated.

3.4.2 Assessing the qualitative and quantitative model implications

Qualitatively, our theory suggests that high disaster probabilities coincide with backwardation. We test this restriction in a logistic regression setting. Suppose $\mathbb{1}_{\{\text{slope of the VIX futures curve}_t>0\}}$ is consistent with a Bernoulli probability function and takes a value of 1 when in contango (with probability $\mathbb{q}_t$) and 0 (when in backwardation) with probability $1-\mathbb{q}_t$. Our empirical specification is the following: $\mathbb{q}_t = (1 + e^{-\{\mathbb{a}_\lambda + \mathbb{b}_\lambda \log(\frac{1}{\boldsymbol{\lambda}_t})\}})^{-1}$. The takeaway from Table 5 (Panel A) is the rejection of $\mathbb{b}_\lambda = 0$ (based on p-values of the z-statistics). The noticeably positive $\mathbb{b}_\lambda$ estimates affirm a qualitative implication of our theory of volatility uncertainty. Specifically, low values of $\boldsymbol{\lambda}_t$ map to VIX futures contango.

On the other hand, the contingency table in Table 5 (Panel B) bears on the quantitative implication of the theory: Joint counts of the shape of the VIX futures curve and realizations of $\boldsymbol{\lambda}_t$ are directionally aligned for 90% (76%+14%) of the weekly observations. The economic states when $\boldsymbol{\lambda}_t$ is higher, or lower, than its long-term mean can be visualized from the plot of demeaned $\log(\boldsymbol{\lambda}_t)$ in the Internet Appendix (Figure I.1). Complementing this evidence, Table 5 (Panel C) shows the features of the extracted $\boldsymbol{\lambda}_t$, and Table 5 (Panel D) provides estimates of the noncentral chi-square transition density function of $\boldsymbol{\lambda}_t$ (as modeled in equation (18)).

3.4.3 Bootstrap confidence intervals for model consistency

We present the 95% confidence intervals (shown as $\lfloor . \rfloor$ in Panel D) for the contingency table, obtained from 5,000 bootstrapped series of a bivariate VAR(1) model for $\boldsymbol{y}_t \equiv [\log(\boldsymbol{\lambda}_t), \log(\frac{F_t^{(2)}}{F_t^{(1)}})]'$, selected by the Bayesian information criterion. As in Bauer and Hamilton (2018), we resort to estimating $\boldsymbol{y}_t = \boldsymbol{\alpha} + \boldsymbol{\beta}\boldsymbol{y}_{t-1} + \boldsymbol{\epsilon}_t$. Then, we jointly bootstrap the residuals and construct $\boldsymbol{y}_t^b = \hat{\boldsymbol{\alpha}} + \hat{\boldsymbol{\beta}}\boldsymbol{y}_{t-1}^b + \boldsymbol{\epsilon}_t^b$ for b=1,...,5000.

Evidenced by the bootstrap confidence intervals, the joint counts of model consistency appear robust to estimation noise in mean disaster probabilities and persistence in the slopes of the VIX futures curve. Overall, our evidence, based on inferring $\boldsymbol{\lambda}_t$ from the price of deep OTM puts on weeklys, is supportive of the economic mechanism that underlies VIX futures contango.

3.5 Stochastic orders of equity volatility uncertainty and alternative approaches

The mechanism underlying stochastic orders of volatility uncertainty can also be studied under the altered modeling approach of (i) a constant disaster probability in the equity price process and (ii) an equity return volatility structure with two *diffusive* components. We frame this question in Internet Appendix (Section A.4), utilizing the model of Bates (2000). Our analysis implies that the sign of $\mathbb{E}^{\mathbb{Q}}(\widetilde{Z}_{T_1}|\mathcal{I}_t) - \mathbb{E}^{\mathbb{Q}}(\widetilde{Z}_{T_2}|\mathcal{I}_t)$ depends on whether the current value of the two equity return volatility components are below, or above, their respective long-run mean levels. Additionally, in this case, the switch from contango to backwardation (or the reverse) is not restricted by the distributional features of equity price jumps.

One may also examine the mechanism of stochastic orders of equity volatility uncertainty under an equilibrium model. In this regard, our models complement the parametric modeling of consumption growth — under the real-world and risk-neutral probability measures — in Eraker and Yang (2020). The variance of consumption growth is parameterized by a diffusive volatility component and a jump component with stochastically evolving jump intensity. Essential to Eraker and Yang (2020) is a pricing kernel with (i) diffusive risks and (ii) jump risks accompanied by stochastic jump intensity. Their approach is to derive the form of the VIX in an equilibrium framework while capturing features of VIX option prices. The connecting aspect of our paper is to identify intertemporal restrictions, namely, the stochastic orders of equity volatility uncertainty, such that the VIX futures curve can transition between contango and backwardation.

4 Conclusion

VIX futures are said to be in contango when progressively longer-dated VIX futures contracts trade at progressively higher prices. While textbook treatments recognize that investment assets are in contango due to a cost-of-carry relation arising from a no-arbitrage condition, it is far from settled why VIX futures — which are hedging instruments — should be upward sloping with maturity.

We feature empirical facts, which also serve as the background for our theory. First, VIX futures are in contango around 82% in our daily sample. Second, despite being *on average* in contango, VIX futures curve exhibits backwardation during periods of heightened economic uncertainties. Third, changes in the slope of the VIX futures curve are not coincident with changes in the slope

of the implied volatility curve for at-the-money S&P 500 options. Fourth, rescaled range analysis implies that VIX is mean-reverting. Fifth, principal component analysis indicates that two factors describe 99.78% of the cross-sectional variation in VIX futures prices. Finally, shorting the VIX futures contract with the most pronounced contango collects positive carry.

Building on our empirical observations, we develop a theory that exploits the notion that short-dated volatility uncertainty is "stochastically smaller" than long-dated volatility uncertainty (under all pricing measures). The device of stochastic orders of volatility uncertainty helps to decode the sufficient conditions for when the VIX futures curve will predominantly be in contango. The advantage of this approach is that it can be complemented with parametric modeling.

Combining our theoretical approach with a parametric model, in conjunction with our empirical evidence, we consider a dynamic model of equity price dynamics that contains both diffusive stochastic volatility risks and jump risks. The latter is relevant to interpreting traded volatility uncertainty and reflects a disaster component with a stochastically varying probability of disasters.

The workings of our model reveal that the VIX futures curve is in contango when investors regard disaster or volatility risks to be low relative to long-run reversion levels. This central intuition holds when jumps in volatility, correlated with price jumps, are allowed. These outcomes are shown to be consistent with our theory of stochastically smaller short-dated volatility uncertainty, a feature that is mirrored pervasively in empirical VIX futures curves.[9]

[9]The pricing of VIX futures contracts is an essential component for the determination of exchange-traded notes on volatility (e.g., VXX (with substantial trading volume)). Thus, the shape of the VIX futures curve merits a broader theoretical understanding.

References

H. Ai, L. Han, and L. Xu. Information-driven volatility. Working paper, Syracuse University, 2021.

Y. Aït-Sahalia and J. Jacod. Analyzing the spectrum of asset returns: Jump and volatility components in high frequency data. *Journal of Econometrics*, 50(4):1007–1050, 2012.

Y. Aït-Sahalia, J. Cacho-Diaz, and R. Laeven. Modeling financial contagion using mutually exciting jump processes. *Journal of Financial Economics*, 117(3):585–606, 2015.

Y. Aït-Sahalia, M. Karaman, and L. Mancini. The term structure of variance swaps and risk premia. *Journal of Econometrics*, 219:204–230, 2020.

Y. Aït-Sahalia, C. Li, and C. X. Li. Implied stochastic volatility models. *Review of Financial Studies*, 34:394–450, 2021.

D. Amengual and D. Xiu. Resolution of policy uncertainty and sudden declines in volatility. *Journal of Econometrics*, 203:297–315, 2018.

T. Andersen, T. Bollerslev, F. Diebold, and P. Labys. Modeling and forecasting realized volatility. *Econometrica*, 71(2):579–625, 2003.

T. Andersen, T. Bollerslev, and F. Diebold. Roughing it up: Including jump components in the measurement. *Review of Economics and Statistics*, 89:701–720, 2007.

G. Bakshi, D. Madan, and G. Panayotov. Heterogeneity in beliefs and volatility tail behavior. *Journal of Financial and Quantitative Analysis*, 50(6):1389–1414, 2015.

G. Bakshi, J. Crosby, and X. Gao. Dark matter in (volatility and) equity option risk premiums. Working paper, Temple University and University of Maryland, 2020.

F. Bandi and R. Reno. Price and volatility co-jumps. *Journal of Financial Economics*, 119:107–146, 2016.

C. Bardgett, E. Gourier, and M. Leippold. The information content of S&P 500 and VIX derivatives markets. *Journal of Financial Economics*, 131:593–618, 2019.

D. Bates. Post-'87 crash fears in the S&P 500 futures option market. *Journal of Econometrics*, 94 (1/2):181–238, 2000.

D. Bates. US stock market crash risk, 1926–2010. *Journal of Financial Economics*, 105(2):229–259, 2012.

M. Bauer and J. Hamilton. Robust bond risk premia. *Review of Financial Studies*, 31(2):399–448, 2018.

T. Bollerslev and V. Todorov. Tails, fears and risk premia. *Journal of Finance*, 66:2165–2211, 2011.

M. Brenner and M. Subrahmanyam. A simple formula to compute the implied standard deviation. *Financial Analysts Journal*, 44(5):80–83, 1988.

M. Broadie and A. Jain. The effect of jumps and discrete sampling on volatility and variance swaps. *International Journal of Theoretical and Applied Finance*, 11(8):761–797, 2008.

P. Carr and R. Lee. Robust replication of volatility derivatives. Working paper, New York University and University of Chicago, 2008.

P. Carr and L. Wu. A tale of two indices. *Journal of Derivatives*, 13:13–29, 2006.

CBOE. VIX: White paper. Working paper, Chicago Board of Options Exchange, 2006.

I. Cheng. The VIX premium. *Review of Financial Studies*, 32(1):180–227, 2019.

R. Cont and T. Kokholm. A consistent pricing model for index options and volatility derivatives. *Mathematical Finance*, 23(2):248–274, 2013.

J. Cox, J. Ingersoll, and S. Ross. A theory of the term structure of interest rates. *Econometrica*, 53(2):385–407, 1985.

I. Dew-Becker, S. Giglio, A. Le, and M. Rodriguez. The price of variance risk. *Journal of Financial Economics*, 123(2):225–250, 2017.

I. Drechsler and A. Yaron. What's vol got to do with it. *Review of Financial Studies*, 24(1):1–45, 2011.

J. Duan and C. Yeh. Jump and volatility risk premiums implied by VIX. *Journal of Economic Dynamics and Control*, 34:2232–2244, 2007.

D. Duffie, J. Pan, and K. Singleton. Transform analysis and asset pricing for affine jump diffusions. *Econometrica*, 68(6):1343–1376, 2000.

B. Eraker and Y. Wu. Explaining the negative returns to volatility claims: An equilibrium approach. *Journal of Financial Economics*, 125(1):72–98, 2017.

B. Eraker and A. Yang. The price of higher order catastrophe insurance: The case of VIX options. Working paper, University of Wisconsin, 2020.

X. Gabaix. Variable rare disasters: An exactly solved framework for ten puzzles in macro-finance. *Quarterly Journal of Economics*, 127:645–700, 2012.

A. Grünbichler and F. Longstaff. Valuing futures and options on volatility. *Journal of Banking and Finance*, 20:985–1001, 1996.

G. Hu and K. Jacobs. Expected and realized returns on volatility. Working paper, University of Sydney and University of Houston, 2020.

D. Huang, C. Schlag, I. Shaliastovich, and J. Thimme. Volatility of volatility risk. *Journal of Financial and Quantitative Analysis*, 18:519–543, 2020.

T. Johnson. Risk premia and the VIX term structure. *Journal of Financial and Quantitative Analysis*, 52:2461–2490, 2017.

S. Kou. A jump-diffusion model for option pricing. *Management Science*, 48:1086–1101, 2002.

Y. Lin and C. Chang. Consistent modeling of S&P 500 and VIX derivatives. *Journal of Economic Dynamics and Control*, 11:2302–2319, 2010.

A. Lo. The long-term memory in stock prices. *Econometrica*, 59(5):1279–1313, 1991.

A. Lo and C. MacKinlay. *A non-random walk down Wall Street*. Princeton University Press, 2011.

L. Lochstoer and T. Muir. Volatility expectations and returns. Working paper, UCLA, 2020.

J. Mencia and E. Sentana. Valuation of VIX derivatives. *Journal of Financial Economics*, 108: 367–391, 2013.

R. Merton. Option pricing when underlying stock returns are discontinuous. *Journal of Financial Economics*, 3(1):125–144, 1976.

S. Mixon and E. Onur. Volatility derivatives in practice: Activity and impact. Working paper, Commodity Futures and Trading Commission, 2018.

W. Newey and K. West. A simple, positive semi-definite, heteroskedasticity and autocorrelation consistent covariance matrix. *Econometrica*, 55(3):703–708, 1987.

Y. Park. The effects of asymmetric volatility and jumps on the pricing of VIX derivatives. *Journal of Econometrics*, 192:313–328, 2016.

N. Privault. *Stochastic Finance: An Introduction with Market Examples*. Chapman and Hall, New York, 2014.

P. Protter. *Stochastic Integration and Differential Equations*. Springer, Berlin, 2013.

S. Ross. *Stochastic Processes*. Wiley, New York, 1984.

P. Santa-Clara and S. Yan. Crashes, volatility, and the equity premium: Lessons from S&P 500 options. *Review of Economics and Statistics*, 92:435–451, 2010.

K. Schürger. Laplace transforms and suprema of stochastic processes. In *Advances in Finance and Stochastics*, volume 1, pages 285–294. Springer, Amsterdam, 2002.

G. Shaked and G. Shantikumar. *Stochastic Orders*. Springer, 2006.

V. Todorov. Variance risk premium dynamics: The role of jumps. *Review of Financial Studies*, 23 (1):345–383, 2010.

V. Todorov and G. Tauchen. Volatility jumps. *Journal of Business & Economic Statistics*, 29(3): 356–371, 2011.

J. Wachter. Can time-varying risk of rare disasters explain aggregate stock market volatility? *Journal of Finance*, 68:987–1035, 2013.

S. Zhu and G. Lian. A closed-form exact solution for pricing variance swaps with stochastic volatility. *Mathematical Finance*, 21(2):233–256, 2011.

Y. Zhu and J. Zhang. Variance term structure and VIX futures pricing. *International Journal of Theoretical and Applied Finance*, 10:111–127, 2007.

Appendix

A Appendix A: Proof of Result 1 (stochastic orders and VIX futures curve)

Postulate $T_1 < T_2 < \ldots < T_n$. We fix the notation as follows:

$\widetilde{Z}_{T_n} = \mathbb{E}^{\mathbb{Q}}(\{-\frac{2}{\hbar}\}\log(\frac{S_{T_n+\hbar}}{H_{T_n}^{T_n+\hbar}})\Big|\mathcal{I}_{T_n}) \in (0,\infty)$ is the price of volatility uncertainty at time T_n.

$\mathbb{G}_{T_n}$ (respectively, $\overline{\mathbb{G}}_{T_n}$) is the distribution function (respectively, complementary distribution function) of $\widetilde{Z}_{T_n}$ under the probability measure $\mathbb{Q}$.

Ross (1984, Chapter 9.1) defines $\widetilde{Z}_{T_1}$ to be *stochastically smaller* than $\widetilde{Z}_{T_2}$, written $\widetilde{Z}_{T_1} \leq_{\text{st}} \widetilde{Z}_{T_2}$, if

$$\overbrace{\overline{\mathbb{G}}_{T_1}[\mathbb{z}]}^{\equiv\ \text{Prob}^{\mathbb{Q}}[\widetilde{Z}_{T_1}\geq \mathbb{z}]} \quad \leq \quad \overbrace{\overline{\mathbb{G}}_{T_2}[\mathbb{z}]}^{\equiv\ \text{Prob}^{\mathbb{Q}}[\widetilde{Z}_{T_2}\geq \mathbb{z}]}, \qquad \text{for all} \quad \mathbb{z}\in(0,\infty). \tag{A1}$$

Then, by Ross (1984, Lemma 9.1.1), it holds that $\mathbb{E}^{\mathbb{Q}}(\widetilde{Z}_{T_1}\big|\mathcal{I}_t) \leq \mathbb{E}^{\mathbb{Q}}(\widetilde{Z}_{T_2}\big|\mathcal{I}_t)$. Furthermore, by Ross (1984, Proposition 9.1.2)

$$\widetilde{Z}_{T_1} \leq_{\text{st}} \widetilde{Z}_{T_2} \qquad \Longleftrightarrow \qquad \mathbb{E}^{\mathbb{Q}}(\mathfrak{f}[\widetilde{Z}_{T_1}]\Big|\mathcal{I}_t) \ \leq\ \mathbb{E}^{\mathbb{Q}}(\mathfrak{f}[\widetilde{Z}_{T_2}]\Big|\mathcal{I}_t), \tag{A2}$$

for all mappings $\mathfrak{f}:\mathbb{R}\to\mathbb{R}$, which are nondecreasing, provided that the expectations exist. Result 1 follows since $\sqrt{\bullet}$ is nondecreasing. ■

B Appendix B: Restrictions on volatility uncertainty in equations (19)–(20) of Section 3

Throughout, $\hbar$ is fixed to 30/365.

In the setup described in equations (14)–(18), the price jumps are modeled as arriving at random times t_j with jump intensity $\boldsymbol{\lambda}_t$, which is itself variable. Thus, we consider $S_{t_j} = S_{t_j-}\, e^{x_j}$ and, therefore, $S_{t_j} - S_{t_j-} = S_{t_j-}\,(e^{x_j}-1)$. Let $\mathbb{E}^{\mathbb{Q}}(\bullet)$ denote unconditional expectation.

Applying Ito's Lemma for semimartingales to (15) and using the fact that $H_t^{t+\hbar} = e^{r\hbar}\, S_t$, we obtain

$$\log(\frac{S_{t+\hbar}}{H_t^{t+\hbar}}) \ =\ -\frac{1}{2}\int_t^{t+\hbar}\mathbf{v}_u\, du + \int_t^{t+\hbar}\sqrt{\mathbf{v}_u}\, d\mathbb{B}_u^{\mathbb{Q},\text{s}} + \sum_{j=\mathbb{N}_t^{\mathbb{Q}}}^{\mathbb{N}_{t+\hbar}^{\mathbb{Q}}} x_j - \underbrace{\int_t^{t+\hbar}\boldsymbol{\lambda}_u\,\mathbb{E}^{\mathbb{Q}}(e^x-1)du}_{\text{compensator}}. \tag{B1}$$

The size of the disasters $-\infty < x < \infty$ is an i.i.d random variable (satisfying $\mathbb{E}^{\mathbb{Q}}(e^x) < \infty$) and is independent of the Poisson process $\mathbb{N}_t^{\mathbb{Q}}$.

We exploit known results to verify the expressions in Section 3.2. First, for some variable y_t, if

$$d\mathrm{y}_t \;=\; (\theta - \kappa\,\mathrm{y}_t)\,dt \;+\; \sigma\,\sqrt{\mathrm{y}_t}\,d\mathbb{B}_t^{\mathbb{Q}}, \tag{B2}$$

$$\text{then} \qquad \mathbb{E}^{\mathbb{Q}}\left(\int_T^{T+\hbar} \mathrm{y}_u du\,\Big|\mathcal{I}_T\right) \;=\; \frac{\hbar\,\theta}{\kappa} + \frac{(1-e^{-\kappa\,\hbar})}{\kappa}\{\mathrm{y}_T - \frac{\theta}{\kappa}\}, \tag{B3}$$

$$\text{and} \quad \mathbb{E}^{\mathbb{Q}}\left(\mathrm{y}_T\big|\mathcal{I}_t\right) \;-\; \frac{\theta}{\kappa} \;=\; (\mathrm{y}_t - \frac{\theta}{\kappa})e^{-\kappa(T-t)}. \tag{B4}$$

Next, for compound Poisson processes (e.g., Privault (2014, Chapter 14.2))

$$\mathbb{E}^{\mathbb{Q}}(\sum_{j=\mathbb{N}_T^{\mathbb{Q}}}^{\mathbb{N}_{T+\hbar}^{\mathbb{Q}}} x_j\Big|\mathcal{I}_T) \;=\; \mathbb{E}^{\mathbb{Q}}(\int_T^{T+\hbar} \boldsymbol{\lambda}_u\,du\Big|\mathcal{I}_T)\;\mathbb{E}^{\mathbb{Q}}(x). \tag{B5}$$

Hence, the price of volatility uncertainty over T and $T+\hbar$ has two sources

$$\begin{aligned}
\widetilde{Z}_T \;&=\; \mathbb{E}^{\mathbb{Q}}(\{-\frac{2}{\hbar}\}\log(\frac{S_{T+\hbar}}{H_T^{T+\hbar}})\Big|\mathcal{I}_T), \\
&=\; \mathbb{E}^{\mathbb{Q}}(\{-\frac{2}{\hbar}\}\{-\frac{1}{2}\underbrace{\int_T^{T+\hbar}\mathbf{v}_u\,du}_{\substack{\text{diffusive volatility risks}\\ \text{over } T \text{ to } T+\hbar}} + \underbrace{\sum_{j=\mathbb{N}_T^{\mathbb{Q}}}^{\mathbb{N}_{T+\hbar}^{\mathbb{Q}}} x_j - \int_T^{T+\hbar}\boldsymbol{\lambda}_u\,\mathbb{E}^{\mathbb{Q}}(e^x-1)\,du\}}_{\substack{\text{disaster risks}\\ \text{over } T \text{ to } T+\hbar}}\Big|\mathcal{I}_T).
\end{aligned} \tag{B6}$$

Evaluate the second term and rearrange using equation (B5)

$$\widetilde{A}_T^{T+\hbar} \;\equiv\; \mathbb{E}^{\mathbb{Q}}\left(\{-\frac{2}{\hbar}\}\{\sum_{j=\mathbb{N}_T^{\mathbb{Q}}}^{\mathbb{N}_{T+\hbar}^{\mathbb{Q}}} x_j - \int_T^{T+\hbar}\boldsymbol{\lambda}_u\,\mathbb{E}^{\mathbb{Q}}(e^x-1)\,du\}\Big|\mathcal{I}_T\right) \tag{B7}$$

$$=\; \{-\frac{2}{\hbar}\}\,\mathbb{E}^{\mathbb{Q}}(\int_T^{T+\hbar}\boldsymbol{\lambda}_u\,du\Big|\mathcal{I}_T)\,\mathbb{E}^{\mathbb{Q}}(x) \;+\; \{\frac{2}{\hbar}\}\mathbb{E}^{\mathbb{Q}}(e^x-1)\,\mathbb{E}^{\mathbb{Q}}(\int_T^{T+\hbar}\boldsymbol{\lambda}_u\,du\Big|\mathcal{I}_T) \tag{B8}$$

$$=\; \frac{2}{\hbar}\{-\mathbb{E}^{\mathbb{Q}}(x)+\mathbb{E}^{\mathbb{Q}}(e^x-1)\}\;\underbrace{\mathbb{E}^{\mathbb{Q}}(\int_T^{T+\hbar}\boldsymbol{\lambda}_u\,du\Big|\mathcal{I}_T)}_{\text{using equation (B3)}} \tag{B9}$$

$$=\; 2\,\underbrace{\{\,\mathbb{E}^{\mathbb{Q}}(e^x-1-x)\}}_{\geq\,0\;\text{(Jensen's inequality)}}\left(\frac{\theta_\lambda}{\kappa_\lambda} + \frac{(1-e^{-\kappa_\lambda\hbar})}{\hbar\,\kappa_\lambda}(\boldsymbol{\lambda}_T - \frac{\theta_\lambda}{\kappa_\lambda})\right). \tag{B10}$$

Note that (by Jensen's inequality) $\mathbb{E}^{\mathbb{Q}}(e^x - 1 - x) \geq 0$ for any (i.i.d.) distribution of jump sizes x satisfying $\mathbb{E}^{\mathbb{Q}}(e^x) < \infty$. For example, one could specify jump sizes that are (i) Gaussian (Merton (1976)) or (ii) double exponential (Kou (2002)).

Returning to equation (B6), it then holds that

$$\widetilde{Z}_T = \frac{1}{\hbar} \underbrace{\mathbb{E}^{\mathbb{Q}}\left(\int_T^{T+\hbar} \mathbf{v}_u du \big| \mathcal{I}_T \right)}_{\text{using equation (B3)}} + \widetilde{A}_T^{T+\hbar} \tag{B11}$$

$$= \frac{\theta_{\text{vol}}}{\kappa_{\text{vol}}} + \frac{(1 - e^{-\kappa_{\text{vol}}\hbar})}{\hbar\,\kappa_{\text{vol}}} \{\mathbf{v}_T - \frac{\theta_{\text{vol}}}{\kappa_{\text{vol}}}\} + \underbrace{\widetilde{A}_T^{T+\hbar}}_{\text{using equation (B10)}}. \tag{B12}$$

The expression presented in equation (19) is deduced.

To obtain an expression for $\mathbb{E}^{\mathbb{Q}}(\widetilde{Z}_T | \mathcal{I}_t)$ employed in equation (20), we note, from equation (B4), that $\mathbb{E}^{\mathbb{Q}}\left(\mathbf{v}_T | \mathcal{I}_t\right) - \frac{\theta_{\text{vol}}}{\kappa_{\text{vol}}} = (\mathbf{v}_t - \frac{\theta_{\text{vol}}}{\kappa_{\text{vol}}}) e^{-\kappa_{\text{vol}}(T-t)}$ and analogously for $\mathbb{E}^{\mathbb{Q}}\left(\boldsymbol{\lambda}_T | \mathcal{I}_t\right) - \frac{\theta_\lambda}{\kappa_\lambda}$. ■

C Appendix C: Model with time-varying disaster probability and co-jumps in price and volatility

We consider the model in (22)-(27) of Section 3.3. This model incorporates (i) time-varying probability of disasters $\boldsymbol{\lambda}_t$ and (ii) co-jumps in equity price and volatility. Volatility has both diffusive and discontinuous components. We reinforce the notion of stochastically smaller short-dated volatility uncertainty when there are co-jumps in price and volatility under time-varying disaster probability.

The departure with volatility jumps and stochastic intensity is that equation (27) implies

$$\mathbb{E}^{\mathbb{Q}}\left(\mathbf{v}_{T+\hbar} | \mathcal{I}_T\right) - \frac{\theta_{\text{vol}}}{\kappa_{\text{vol}}} = (\mathbf{v}_T - \frac{\theta_{\text{vol}}}{\kappa_{\text{vol}}}) e^{-\kappa_{\text{vol}}\hbar} + \mathbb{E}^{\mathbb{Q}}(x_{\mathbf{v}})\, \mathbb{E}^{\mathbb{Q}}(\int_T^{T+\hbar} \boldsymbol{\lambda}_u\, e^{\kappa_{\text{vol}}(u-T-\hbar)} du | \mathcal{I}_T). \tag{C1}$$

We note that volatility jumps are additive with $\mathbb{E}^{\mathbb{Q}}(x_{\mathbf{v}}) > 0$. The consequence of integrating $d\mathbf{v}_t = (\theta_{\text{vol}} - \kappa_{\text{vol}}\mathbf{v}_t)dt + \sigma_{\text{vol}}\sqrt{\mathbf{v}_t} d\mathbb{B}_t^{\mathbb{Q},\mathbf{v}} + x_{\mathbf{v}} d\mathbb{N}_t^{\mathbb{Q}}$, taking expectation, and using (C1), is the following:

$$\mathbb{E}^{\mathbb{Q}}(\int_T^{T+\hbar} \mathbf{v}_u\, du | \mathcal{I}_T) = \frac{\theta_{\text{vol}}}{\kappa_{\text{vol}}}\hbar + \frac{1}{\kappa_{\text{vol}}}(\mathbf{v}_T - \frac{\theta_{\text{vol}}}{\kappa_{\text{vol}}})\{1 - e^{-\kappa_{\text{vol}}\hbar}\}$$
$$+ \frac{\mathbb{E}^{\mathbb{Q}}(x_{\mathbf{v}})}{\kappa_{\text{vol}}} \int_T^{T+\hbar} \underbrace{\mathbb{E}^{\mathbb{Q}}(\boldsymbol{\lambda}_u | \mathcal{I}_T)}_{\mathbb{E}^{\mathbb{Q}}(\boldsymbol{\lambda}_u | \mathcal{I}_T) - \frac{\theta_\lambda}{\kappa_\lambda} = (\boldsymbol{\lambda}_T - \frac{\theta_\lambda}{\kappa_\lambda}) e^{-\kappa_\lambda (u-T)}} \{1 - e^{\kappa_{\text{vol}}(u-T-\hbar)}\} du. \tag{C2}$$

The price of volatility uncertainty over T and $T+\hbar$ still has two sources that are time-varying:

$$\widetilde{Z}_T \;=\; \mathbb{E}^{\mathbb{Q}}(\{-\frac{2}{\hbar}\}\{-\frac{1}{2}\underbrace{\int_T^{T+\hbar}\mathbf{v}_u\,du}_{\substack{\text{volatility risks}\\ \text{over } T \text{ to } T+\hbar}} \;+\; \underbrace{\sum_{j=\mathbb{N}_T^{\mathbb{Q}}}^{\mathbb{N}_{T+\hbar}^{\mathbb{Q}}} x_{s_j} - \int_T^{T+\hbar}\boldsymbol{\lambda}_u\,\mathbb{E}^{\mathbb{Q}}(e^{x_s}-1)\,du\}}_{\substack{\text{disaster risks}\\ \text{over } T \text{ to } T+\hbar}}\Big|\mathcal{I}_T). \tag{C3}$$

Organizing the next step, we note that

$$\begin{aligned}\widetilde{A}_T^{T+\hbar} \;&\equiv\; \mathbb{E}^{\mathbb{Q}}\left(\{-\frac{2}{\hbar}\}\{\sum_{j=\mathbb{N}_T^{\mathbb{Q}}}^{\mathbb{N}_{T+\hbar}^{\mathbb{Q}}} x_{s_j} - \int_T^{T+\hbar}\boldsymbol{\lambda}_u\,\mathbb{E}^{\mathbb{Q}}(e^{x_s}-1)\,du\}\Big|\mathcal{I}_T\right)\\ &=\; 2\,\underbrace{\{\mathbb{E}^{\mathbb{Q}}(e^{x_s}-1-x_s)\}}_{\geq\,0\ \text{(Jensen's inequality)}}\left(\frac{\theta_\lambda}{\kappa_\lambda}+\frac{(1-e^{-\kappa_\lambda\hbar})}{\hbar\,\kappa_\lambda}(\boldsymbol{\lambda}_T-\frac{\theta_\lambda}{\kappa_\lambda})\right).\end{aligned} \tag{C4}$$

Returning to equation (C3) and using the form of (C2), it then holds that

$$\widetilde{Z}_T \;=\; \frac{1}{\hbar}\underbrace{\mathbb{E}^{\mathbb{Q}}\left(\int_T^{T+\hbar}\mathbf{v}_u du\big|\mathcal{I}_T\right)}_{\text{using equation (C2)}} \;+\; \widetilde{A}_T^{T+\hbar} \tag{C5}$$

$$\begin{aligned}&=\; \frac{\theta_{\text{vol}}}{\kappa_{\text{vol}}}+\frac{(1-e^{-\kappa_{\text{vol}}\,\hbar})}{\hbar\,\kappa_{\text{vol}}}\{\mathbf{v}_T-\frac{\theta_{\text{vol}}}{\kappa_{\text{vol}}}\}\\ &\quad+\; \underbrace{\frac{\mathbb{E}^{\mathbb{Q}}(x_{\mathbf{v}})}{\hbar\,\kappa_{\text{vol}}}\int_T^{T+\hbar}\left(\frac{\theta_\lambda}{\kappa_\lambda}+(\boldsymbol{\lambda}_T-\frac{\theta_\lambda}{\kappa_\lambda})e^{-\kappa_\lambda(u-T)}\right)(1-e^{\kappa_{\text{vol}}(u-T-\hbar)})\,du}_{\text{expanding from (C2)}} \;+\; \underbrace{\widetilde{A}_T^{T+\hbar}}_{\text{using (C4)}}.\end{aligned} \tag{C6}$$

To obtain $\mathbb{E}^{\mathbb{Q}}(\widetilde{Z}_{T_1}|\mathcal{I}_t)-\mathbb{E}^{\mathbb{Q}}(\widetilde{Z}_{T_2}|\mathcal{I}_t)$ in equation (28), we use equation (C6) twice — once to get $\mathbb{E}^{\mathbb{Q}}(\widetilde{Z}_{T_1}|\mathcal{I}_t)$ and next to get $\mathbb{E}^{\mathbb{Q}}(\widetilde{Z}_{T_2}|\mathcal{I}_t)$ — then we subtract and rearrange.

Specifically,

$$\begin{aligned}\mathbb{E}^{\mathbb{Q}}(\widetilde{Z}_T|\mathcal{I}_t) \;&=\; \frac{\theta_{\text{vol}}}{\kappa_{\text{vol}}}+\frac{(1-e^{-\kappa_{\text{vol}}\,\hbar})}{\hbar\,\kappa_{\text{vol}}}\underbrace{\mathbb{E}^{\mathbb{Q}}(\{\mathbf{v}_T-\frac{\theta_{\text{vol}}}{\kappa_{\text{vol}}}\}|\mathcal{I}_t)}_{\text{substitute from (C8)}}\\ &\quad+\; \frac{\mathbb{E}^{\mathbb{Q}}(x_{\mathbf{v}})}{\hbar\,\kappa_{\text{vol}}}\int_T^{T+\hbar}\left(\frac{\theta_\lambda}{\kappa_\lambda}\;+\;\mathbb{E}^{\mathbb{Q}}(\{\boldsymbol{\lambda}_T-\frac{\theta_\lambda}{\kappa_\lambda}\}|\mathcal{I}_t)\,e^{-\kappa_\lambda(u-T)}\right)(1-e^{\kappa_{\text{vol}}(u-T-\hbar)})du\\ &\quad+\; \mathbb{E}^{\mathbb{Q}}(\widetilde{A}_T^{T+\hbar}|\mathcal{I}_t).\end{aligned} \tag{C7}$$

Term 4 in equation (28) is determined from $\mathbb{E}^{\mathbb{Q}}(\widetilde{A}_{T_1}^{T_1+\hbar}|\mathcal{I}_t)-\mathbb{E}^{\mathbb{Q}}(\widetilde{A}_{T_2}^{T_2+\hbar}|\mathcal{I}_t)$.

For our purposes, we additionally recognize that

$$\mathbb{E}^{\mathbb{Q}}(\mathbf{v}_T\big|\mathcal{I}_t) - \frac{\theta_{\text{vol}}}{\kappa_{\text{vol}}} = (\mathbf{v}_t - \frac{\theta_{\text{vol}}}{\kappa_{\text{vol}}})\, e^{-\kappa_{\text{vol}}(T-t)} \;+\; \mathbb{E}^{\mathbb{Q}}(x_{\mathbf{v}})\, \mathbb{E}^{\mathbb{Q}}(\int_t^T \boldsymbol{\lambda}_u\, e^{-\kappa_{\text{vol}}(T-u)} du\big|\mathcal{I}_t). \tag{C8}$$

With $\mathbb{E}^{\mathbb{Q}}(\widetilde{Z}_T\big|\mathcal{I}_t)$ outlined, we first show how Term 1 and Term 2 of equation (28) are obtained. It follows that

$$\begin{aligned}\mathbb{E}^{\mathbb{Q}}(\int_t^T \boldsymbol{\lambda}_u e^{-\kappa_{\text{vol}}(T-u)}\, du\big|\mathcal{I}_t) &= \int_t^T \left(\frac{\theta_\lambda}{\kappa_\lambda} + e^{-\kappa_\lambda(u-t)}(\boldsymbol{\lambda}_t - \frac{\theta_\lambda}{\kappa_\lambda})\right) e^{-\kappa_{\text{vol}}(T-u)}\, du \\ &= \frac{\theta_\lambda}{\kappa_\lambda}\frac{1-e^{-\kappa_{\text{vol}}(T-t)}}{\kappa_{\text{vol}}} - (\boldsymbol{\lambda}_t - \frac{\theta_\lambda}{\kappa_\lambda})\frac{e^{-\kappa_{\text{vol}}(T-t)} - e^{-\kappa_\lambda(T-t)}}{\kappa_{\text{vol}} - \kappa_\lambda}. \end{aligned} \tag{C9}$$

Accordingly, we note that Term 1 and Term 2 corresponding to $\mathbb{E}^{\mathbb{Q}}(\widetilde{Z}_{T_1}\big|\mathcal{I}_t) - \mathbb{E}^{\mathbb{Q}}(\widetilde{Z}_{T_2}\big|\mathcal{I}_t)$ is

$$\begin{aligned}&\frac{(1-e^{-\kappa_{\text{vol}}\hbar})}{\hbar\,\kappa_{\text{vol}}}\mathbb{E}^{\mathbb{Q}}(x_{\mathbf{v}})\,\{\mathbb{E}^{\mathbb{Q}}(\int_t^{T_1} \boldsymbol{\lambda}_u e^{-\kappa_{\text{vol}}(T_1-u)}\, du - \int_t^{T_2} \boldsymbol{\lambda}_u e^{-\kappa_{\text{vol}}(T_2-u)}\, du\big|\mathcal{I}_t)\} \;= \\ &\underbrace{-\frac{(1-e^{-\kappa_{\text{vol}}\hbar})}{\hbar\,\kappa_{\text{vol}}}\mathbb{E}^{\mathbb{Q}}(x_{\mathbf{v}})\frac{\theta_\lambda}{\kappa_\lambda}\frac{e^{-\kappa_{\text{vol}}(T_1-t)} - e^{-\kappa_{\text{vol}}(T_2-t)}}{\kappa_{\text{vol}}}}_{=\text{ Term 1}} \\ &\underbrace{-\frac{(1-e^{-\kappa_{\text{vol}}\hbar})}{\hbar\,\kappa_{\text{vol}}}\mathbb{E}^{\mathbb{Q}}(x_{\mathbf{v}})\left(\frac{e^{-\kappa_{\text{vol}}(T_1-t)} - e^{-\kappa_\lambda(T_1-t)} - e^{-\kappa_{\text{vol}}(T_2-t)} + e^{-\kappa_\lambda(T_2-t)}}{\kappa_{\text{vol}} - \kappa_\lambda}\right)}_{=\text{ Term 2}}(\boldsymbol{\lambda}_t - \frac{\theta_\lambda}{\kappa_\lambda}). \end{aligned} \tag{C10}$$

In light of component terms in $\mathbb{E}^{\mathbb{Q}}(\widetilde{Z}_T\big|\mathcal{I}_t)$, next we show how Term 3 of equation (28) follows from equation (C6). In this regard, the integral in equation (C6) simplifies as follows:

$$\begin{aligned}&\int_T^{T+\hbar} \left(\frac{\theta_\lambda}{\kappa_\lambda} + (\boldsymbol{\lambda}_T - \frac{\theta_\lambda}{\kappa_\lambda})e^{-\kappa_\lambda(u-T)}\right)(1 - e^{\kappa_{\text{vol}}(u-T-\hbar)})\, du \\ &= \Big[\frac{\theta_\lambda}{\kappa_\lambda}u - \frac{\theta_\lambda}{\kappa_\lambda\kappa_{\text{vol}}}e^{\kappa_{\text{vol}}(u-T-\hbar)} - (\boldsymbol{\lambda}_T - \frac{\theta_\lambda}{\kappa_\lambda})\frac{e^{-\kappa_\lambda(u-T)}}{\kappa_\lambda} \\ &\quad - (\boldsymbol{\lambda}_T - \frac{\theta_\lambda}{\kappa_\lambda})\frac{e^{-\kappa_{\text{vol}}\hbar}}{(\kappa_{\text{vol}} - \kappa_\lambda)}\, e^{(\kappa_{\text{vol}}-\kappa_\lambda)(u-T)}\Big]_{u=T}^{u=T+\hbar} \\ &= \frac{\theta_\lambda}{\kappa_\lambda}\hbar - \frac{\theta_\lambda}{\kappa_\lambda\,\kappa_{\text{vol}}}(1-e^{-\kappa_{\text{vol}}\hbar}) + (\boldsymbol{\lambda}_T - \frac{\theta_\lambda}{\kappa_\lambda})\big(\frac{(1-e^{-\kappa_\lambda\hbar})}{\kappa_\lambda} + \frac{e^{-\kappa_{\text{vol}}\hbar}}{(\kappa_{\text{vol}} - \kappa_\lambda)} - \frac{e^{-\kappa_\lambda\hbar}}{(\kappa_{\text{vol}} - \kappa_\lambda)}\big) \\ &= \frac{\theta_\lambda}{\kappa_\lambda}\hbar - \frac{\theta_\lambda}{\kappa_\lambda\,\kappa_{\text{vol}}}(1-e^{-\kappa_{\text{vol}}\hbar}) \;+\; \big(\frac{e^{-\kappa_{\text{vol}}\hbar} - e^{-\kappa_\lambda\hbar}}{(\kappa_{\text{vol}} - \kappa_\lambda)} \;+\; \frac{(1-e^{-\kappa_\lambda\hbar})}{\kappa_\lambda}\big)(\boldsymbol{\lambda}_T - \frac{\theta_\lambda}{\kappa_\lambda}). \end{aligned} \tag{C11}$$

With this intermediate integration step clarified, we deduce

$$\{\mathbb{E}^{\mathbb{Q}}(\widetilde{Z}_{T_1}|\mathcal{I}_t) - \mathbb{E}^{\mathbb{Q}}(\widetilde{Z}_{T_2}|\mathcal{I}_t)\}\big(\frac{\hbar\,\kappa_{\text{vol}}}{\mathbb{E}^{\mathbb{Q}}(x_{\mathbf{v}})}\big) \;\text{ portion of Term 3 in equation (28)}$$
$$= \frac{\theta_\lambda}{\kappa_\lambda}\hbar - \frac{\theta_\lambda}{\kappa_\lambda\,\kappa_{\text{vol}}}(1-e^{-\kappa_{\text{vol}}\hbar}) + \big(\frac{e^{-\kappa_{\text{vol}}\hbar}-e^{-\kappa_\lambda\hbar}}{(\kappa_{\text{vol}}-\kappa_\lambda)} + \frac{(1-e^{-\kappa_\lambda\hbar})}{\kappa_\lambda}\big)\mathbb{E}^{\mathbb{Q}}(\{\boldsymbol{\lambda}_{T_1} - \frac{\theta_\lambda}{\kappa_\lambda}|\mathcal{I}_t\})$$
$$- \{\frac{\theta_\lambda}{\kappa_\lambda}\hbar - \frac{\theta_\lambda}{\kappa_\lambda\,\kappa_{\text{vol}}}(1-e^{-\kappa_{\text{vol}}\hbar})\} + \big(\frac{e^{-\kappa_{\text{vol}}\hbar}-e^{-\kappa_\lambda\hbar}}{(\kappa_{\text{vol}}-\kappa_\lambda)} + \frac{(1-e^{-\kappa_\lambda\hbar})}{\kappa_\lambda}\big)\mathbb{E}^{\mathbb{Q}}(\{\boldsymbol{\lambda}_{T_2} - \frac{\theta_\lambda}{\kappa_\lambda}|\mathcal{I}_t\}). \quad \text{(C12)}$$

Then substitute $\mathbb{E}^{\mathbb{Q}}\left(\boldsymbol{\lambda}_{T_1}|\mathcal{I}_t\right) - \frac{\theta_\lambda}{\kappa_\lambda} = (\boldsymbol{\lambda}_t - \frac{\theta_\lambda}{\kappa_\lambda})e^{-\kappa_\lambda(T_1-t)}$ and $\mathbb{E}^{\mathbb{Q}}\left(\boldsymbol{\lambda}_{T_2}|\mathcal{I}_t\right) - \frac{\theta_\lambda}{\kappa_\lambda} = (\boldsymbol{\lambda}_t - \frac{\theta_\lambda}{\kappa_\lambda})e^{-\kappa_\lambda(T_2-t)}$. Additionally cancel the constant term $\{\frac{\theta_\lambda}{\kappa_\lambda}\hbar - \frac{\theta_\lambda}{\kappa_\lambda\,\kappa_{\text{vol}}}(1-e^{-\kappa_{\text{vol}}\hbar})\}$. Hence, we obtain the expression displayed as Term 3 in equation (28). □

This was the final step. ■

Table 1: **Contango feature of the VIX futures curve**

Reported results are based on daily VIX futures settlement prices over the sample period from 04/25/2006 to 12/31/2019. Obtained from the CBOE, the data contains open, high, low, close, and settlement prices for VIX futures. The starting date coincides with daily futures prices being available for at least six consecutive VIX futures maturities. There are 3,447 daily observations. We compute the slope (in decimal units) as follows:

$$\text{Slope}_t^{(n)} = \log(\frac{F_t^{(n)}}{F_t^{(1)}}), \qquad \text{for } n = 2, \ldots, 6.$$

Our results in Panel B are based on the following daily regressions:

$$\log(F_t^{(n)}) \;=\; \alpha_t \;+\; \beta_t \, \log(\mathcal{T}_t^{(n)}) \;+\; \epsilon_t^{(n)}, \qquad \text{for } n = 1, \ldots, 6, \text{ and } t = 1, \ldots, \mathbb{T},$$

where $\mathcal{T}_t^{(n)}$ denotes the remaining term-to-maturity (in days) corresponding to futures contract n on day t. We do not report intercept (α). The "t-stat." on β (in Panel B) is obtained by using the HAC estimator of Newey and West (1987). $\mathbb{1}_{\{\text{Slope}_t^{(n)}>0\}}$ is the fraction (in %) of the observations with positive slopes. The row "# NW[t]>2" (Panel B) provides a count of the number of t-statistics for β_t that are higher than 2.0, whereas "# NW[t]< -2" provides a count of the number of t-statistics for β_t that are more negative than -2.0. SD is standard deviation.

Panel A: Contango based on six consecutive VIX futures contracts

	Mean	$\mathbb{1}_{\{\text{Slope}_t^{(n)}>0\}}$ (%)	SD	Min.	Max.	Percentiles 5th	25th	50th	75th	95th
$\log(F_t^{(2)}/F_t^{(1)})$	**0.052**	**81.2**	0.067	-0.401	0.291	-0.061	0.015	0.062	0.096	0.144
$\log(F_t^{(3)}/F_t^{(1)})$	**0.083**	**81.8**	0.101	-0.588	0.388	-0.094	0.027	0.099	0.151	0.218
$\log(F_t^{(4)}/F_t^{(1)})$	**0.104**	**82.0**	0.123	-0.610	0.432	-0.119	0.034	0.124	0.191	0.270
$\log(F_t^{(5)}/F_t^{(1)})$	**0.122**	**82.1**	0.140	-0.621	0.483	-0.131	0.040	0.144	0.222	0.308
$\log(F_t^{(6)}/F_t^{(1)})$	**0.136**	**82.0**	0.154	-0.671	0.547	-0.140	0.042	0.160	0.247	0.339

Panel B: Daily regressions of VIX futures prices

$$\log(F_t^{(n)}) = \alpha_t + \beta_t \, \log(\mathcal{T}_t^{(n)}) + \epsilon_t^{(n)}$$

	Mean	$\mathbb{1}_{\{\beta_t>0\}}$ (%)	SD	Min.	Max.	Percentiles 5th	25th	50th	75th	95th
β	**0.054**	**82.3**	0.062	-0.246	0.229	-0.056	0.016	0.061	0.097	0.141
(t-stat.)	(8.9)									
# NW[t]>2	2702									
# NW[t]< -2	537									

Table 2: **Economic states and shape of the VIX futures curve**

The contango feature of VIX futures is depicted across economic states. The economic state is bracketed by daily VIX (Panel A) or daily S&P 500 index returns (Panel B). All reported results are based on daily VIX futures prices over 04/25/2006 to 12/31/2019. We compute the slope of the VIX futures curve (in decimal units) as $\text{Slope}_t^{(n)} = \log(\frac{F_t^{(n)}}{F_t^{(1)}})$, for $n = 2, \ldots, 6$. Reported $\mathbb{1}_{\{\text{Slope}_t^{(n)}>0\}}$ is the fraction (in %) of the observations with positive slopes.

Panel A: The market state is daily VIX

	Lower VIX	< 10	10	13	15	18	22	30	40	> 50
	Upper VIX		13	15	18	22	30	40	50	
	Frequency (days)	63	712	623	674	549	525	160	84	56
	Frequency (%)	1.8	20.7	18.1	19.6	15.9	15.2	4.6	2.4	1.6
$\log(\frac{F_t^{(2)}}{F_t^{(1)}})$	Mean	0.108	0.092	0.072	0.061	0.044	0.023	-0.033	-0.044	-0.143
	$\mathbb{1}_{\{\text{Slope}_t^{(2)}>0\}}$ (%)	**100**	**99.6**	**98.4**	**91.4**	**72.9**	**62.3**	**35.0**	**14.3**	**1.8**
$\log(\frac{F_t^{(3)}}{F_t^{(1)}})$	Mean	0.175	0.152	0.117	0.101	0.072	0.029	-0.050	-0.094	-0.227
	$\mathbb{1}_{\{\text{Slope}_t^{(3)}>0\}}$ (%)	**100**	**100**	**99.0**	**95.4**	**73.4**	**62.5**	**31.8**	**1.19**	**0**
$\log(\frac{F_t^{(4)}}{F_t^{(1)}})$	Mean	0.237	0.194	0.147	0.130	0.088	0.029	-0.060	-0.125	-0.288
	$\mathbb{1}_{\{\text{Slope}_t^{(4)}>0\}}$ (%)	**100**	**100**	**99.5**	**95.5**	**76.1**	**61.1**	**29.4**	**0**	**0**
$\log(\frac{F_t^{(5)}}{F_t^{(1)}})$	Mean	0.274	0.227	0.171	0.154	0.102	0.029	-0.061	-0.148	-0.335
	$\mathbb{1}_{\{\text{Slope}_t^{(5)}>0\}}$ (%)	**100**	**100**	**99.5**	**96.7**	**77.8**	**59.2**	**28.1**	**0**	**0**
$\log(\frac{F_t^{(6)}}{F_t^{(1)}})$	Mean	0.313	0.254	0.192	0.174	0.111	0.030	-0.064	-0.163	-0.376
	$\mathbb{1}_{\{\text{Slope}_t^{(6)}>0\}}$ (%)	**100**	**100**	**99.5**	**97.9**	**78.5**	**59.2**	**19.4**	**0**	**0**

Panel B: The market state is daily S&P 500 equity index returns

	Return	< -0.035	-0.035	-0.025	-0.015	-0.005	0.005	0.015	0.025	>0.035
	Interval		-0.025	-0.015	-0.005	0.005	0.015	0.025	0.035	
	Frequency (days)	33	55	160	494	1781	714	144	34	31
	Frequency (%)	1.0	1.6	4.6	14.3	51.7	20.7	4.2	1.0	0.9
$\log(\frac{F_t^{(2)}}{F_t^{(1)}})$	Mean	-0.123	-0.037	-0.003	0.033	0.070	0.059	0.021	0.001	-0.077
	$\mathbb{1}_{\{\text{Slope}_t^{(2)}>0\}}$ (%)	**0**	**25.5**	**48.8**	**74.1**	**91.1**	**84.0**	**65.3**	**52.9**	**12.9**
$\log(\frac{F_t^{(3)}}{F_t^{(1)}})$	Mean	-0.182	-0.059	-0.003	0.054	0.113	0.093	0.035	-0.008	-0.131
	$\mathbb{1}_{\{\text{Slope}_t^{(3)}>0\}}$ (%)	**0**	**29.1**	**49.4**	**74.7**	**91.7**	**85.0**	**65.3**	**47.1**	**12.9**
$\log(\frac{F_t^{(4)}}{F_t^{(1)}})$	Mean	-0.223	-0.074	-0.002	0.068	0.143	0.115	0.045	-0.020	-0.167
	$\mathbb{1}_{\{\text{Slope}_t^{(4)}>0\}}$ (%)	**0**	**27.3**	**49.4**	**75.9**	**91.9**	**84.9**	**66.0**	**44.1**	**12.9**
$\log(\frac{F_t^{(5)}}{F_t^{(1)}})$	Mean	-0.254	-0.084	0.000	0.082	0.166	0.133	0.052	-0.022	-0.194
	$\mathbb{1}_{\{\text{Slope}_t^{(5)}>0\}}$ (%)	**0**	**27.3**	**50.6**	**76.7**	**91.9**	**84.7**	**65.3**	**47.0**	**12.9**
$\log(\frac{F_t^{(6)}}{F_t^{(1)}})$	Mean	-0.269	-0.090	0.002	0.093	0.185	0.147	0.058	-0.027	-0.213
	$\mathbb{1}_{\{\text{Slope}_t^{(6)}>0\}}$ (%)	**0**	**27.3**	**49.4**	**77.5**	**92.0**	**84.5**	**63.9**	**41.8**	**12.9**

Table 3: **Slope of the VIX futures curve and slope of the volatility curve of at-the-money S&P 500 index options**

Each day in our sample, we construct the volatilities based on the at-the-money (ATM) S&P 500 index option contracts with *expiration dates* nearest to the corresponding VIX futures contracts. Specifically,

$\mathrm{IV}^{(n)}_{t,\mathrm{spx}}$ is the average of (Black-Scholes) volatility extracted from ATM put and call on the S&P 500 index.

Each day, we compute $\log(\mathrm{IV}^{(2)}_{t,\mathrm{spx}}/\mathrm{IV}^{(1)}_{t,\mathrm{spx}})$ and $\log(\mathrm{IV}^{(4)}_{t,\mathrm{spx}}/\mathrm{IV}^{(1)}_{t,\mathrm{spx}})$. In our calculations

$$\Delta\mathrm{Slope}^{(n)}_{t,\text{spx options}} \equiv \log\left(\frac{\mathrm{IV}^{(n)}_{t,\mathrm{spx}}}{\mathrm{IV}^{(1)}_{t,\mathrm{spx}}}\right) - \log\left(\frac{\mathrm{IV}^{(n)}_{t-1,\mathrm{spx}}}{\mathrm{IV}^{(1)}_{t-1,\mathrm{spx}}}\right) \quad \text{and}$$

$$\Delta\mathrm{Slope}^{(n)}_{t,\text{vix futures}} \equiv \log\left(\frac{F^{(n)}_{t}}{F^{(1)}_{t}}\right) - \log\left(\frac{F^{(n)}_{t-1}}{F^{(1)}_{t-1}}\right).$$

$\Delta\mathrm{Slope}^{(n)}_{t,\text{vix futures}}$	$\Delta\mathrm{Slope}^{(n)}_{t,\text{spx options}}$	Joint frequencies (%) $n=2$	$n=4$
+	+	31	31
−	−	33	32
+	−	**24**	**22**
−	+	**12**	**14**

Table 4: **Weekly excess returns obtained by rank-ordering the VIX futures contracts by the degree of $\frac{F_t^{(n)}}{F_t^{(n-1)}}$**

We employ the following procedure to obtain the returns of contango-sorted VIX futures positions:

step 1. At the end of each Tuesday, compute the slope of the VIX futures curve at six distinct points: $\frac{F_t^{(1)}}{F_t^{(0)}}$, $\frac{F_t^{(2)}}{F_t^{(1)}}$, $\frac{F_t^{(3)}}{F_t^{(2)}}$, $\frac{F_t^{(4)}}{F_t^{(3)}}$, $\frac{F_t^{(5)}}{F_t^{(4)}}$, $\frac{F_t^{(6)}}{F_t^{(5)}}$. These VIX futures contracts are differentiated by expiration dates.

step 2. Sort the VIX futures contracts of different expiration dates from the lowest $\frac{F_t^{(n)}}{F_t^{(n-1)}}$ to the highest. Compute the subsequent weekly VIX futures returns (Tuesday to Tuesday) of a fully collateralized long position, that is $r_{\{t\to t+1\}} = \frac{1}{F_t}(F_{t+1} - F_t)$. The return of the carry — obtained by longing the futures contract of the maturity exhibiting the least contango (lowest $\frac{F_t^{(n)}}{F_t^{(n-1)}}$) and shorting the futures contract of the maturity exhibiting the most contango (highest $\frac{F_t^{(n)}}{F_t^{(n-1)}}$) — is computed as follows:

$$\underbrace{\text{carry}_{\{t\to t+1\}}}_{\text{weekly return}} = \frac{1}{2}(r^{\text{least contangoed}}_{\{t\to t+1\}} - r^{\text{most contangoed}}_{\{t\to t+1\}}).$$

We assign 1/2 dollar to both the long and short legs of the trade.

step 3. Repeat the procedure for each of the 743 weeks (5/23/2006 to 8/11/2020). These returns are rank-ordered by $\frac{F_t^{(n)}}{F_t^{(n-1)}}$.

Reported is the (weekly) mean return, the standard deviation, the percentiles, and the lower and upper 95% i.i.d. bootstrap confidence intervals. ACF_ℓ is the ℓ-order autocorrelation of weekly returns.

	Weekly excess returns of VIX futures contracts (Sorted by lowest $\frac{F_t^{(n)}}{F_t^{(n-1)}}$ to highest $\frac{F_t^{(n)}}{F_t^{(n-1)}}$)						
Groups	1	2	3	4	5	6	$\text{carry}_{\{t\to t+1\}}$ (1 minus 6)/2
	Summary statistics (weekly returns)						
Mean	0.0015	-0.0014	-0.0041	-0.0036	-0.0063	-0.0072	**0.0044**
SD	0.0831	0.0638	0.0627	0.0610	0.0705	0.0778	0.0310
2.5^{th} percentile	-0.1441	-0.1107	-0.1079	-0.1019	-0.1236	-0.1185	-0.0559
50^{th} percentile	-0.0059	-0.0063	-0.0086	-0.0097	-0.0125	-0.0154	0.0050
97.5^{th} percentile	0.1992	0.1455	0.1305	0.1280	0.1480	0.1778	0.0592
ACF_1	0.078	0.055	0.047	0.019	0.012	0.019	0.011
ACF_{12}	0.013	0.031	0.022	0.009	0.025	0.040	-0.056
	Bootstrap confidence intervals on the mean of weekly returns						
Bootstrap lower 95% CI	-0.0042	-0.0058	-0.0084	-0.0079	-0.0114	-0.0127	**0.0022**
Bootstrap upper 95% CI	0.0075	0.0032	0.0005	0.0008	-0.0011	-0.0015	**0.0066**

Table 5: **Qualitative and quantitative implications of the theory**

We employ equation (29) to extract the risk-neutral disaster probability over 519 weeks in our sample of weekly put options (every Friday) from 1/7/2011 to 12/18/2020. There are 76 puts (on average) with non-zero bids for each weekly option cycle and the average moneyness for the deepest OTM put is 23%. Panel A sets up a logistic regression. Let $\mathbb{1}_{\{\text{slope of the VIX futures curve}_t>0\}}$ follow a Bernoulli probability function, which takes a value of 1 when in contango (with probability $\mathbb{q}_t$) and 0 (when in backwardation) with probability $1-\mathbb{q}_t$. The empirical specification is $\mathbb{q}_t = (1+e^{-\{\mathbb{a}_\lambda+\mathbb{b}_\lambda \log(\frac{1}{\boldsymbol{\lambda}_t})\}})^{-1}$. We show the pseudo R^2. Reported alongside is the likelihood ratio (LR), which is distributed $\chi^2(1)$. The p-values for the coefficients ($\mathbb{a}_\lambda$, $\mathbb{b}_\lambda$) are based on z-statistics. Panel B presents a contingency table for the joint counts of the slope of the VIX futures curve and instances that disaster probabilities are greater or less than the estimated long run mean. Reported in $\lfloor . \rfloor$ are the 95% bootstrap lower and upper confidence intervals from a circular block bootstrap. Reported in Panel C are the properties of $\boldsymbol{\lambda}_t$. We show the mean, the standard deviation (SD), the lower and upper 95% bootstrap confidence intervals, the percentiles, and the minimum and the maximum. ACF_1 is the first-order autocorrelation. Panel D reports the maximum likelihood estimation (MLE) of equation (18): $d\boldsymbol{\lambda}_t = \kappa_\lambda(\frac{\theta_\lambda}{\kappa_\lambda} - \boldsymbol{\lambda}_t)dt + \sigma_\lambda\sqrt{\boldsymbol{\lambda}_t}\, d\mathbb{B}_t^{\mathbb{Q},\boldsymbol{\lambda}}$. The transition density follows a non-central chi-square distribution (e.g., Cox, Ingersoll, and Ross (1985, equation (18))).

Panel A: Estimates from the logistic regression

	$\mathbb{a}_\lambda$	p-val.	$\mathbb{b}_\lambda$	p-val.	pseudo-R^2	LR	$\chi^2(1)$ p-val.
$>$ 8% disaster probability	-9.89	{0.00}	2.56	{0.00}	0.56	253	0.00
$>$ 10% disaster probability	-11.19	{0.00}	2.47	{0.00}	0.56	256	0.00

Panel B: Model-implied counts of VIX futures contango and backwardation

	$>$ 8% disaster probability **Count**		$>$ 10% disaster probability **Count**	
	(weeks)	(%)	(weeks)	(%)
Extracted $\boldsymbol{\lambda}_t <$ estimated $\frac{\theta_\lambda}{\kappa_\lambda}$ and VIX futures in contango	**396**	**76**	**402**	**77**
	$\lfloor$350, 411$\rfloor$	$\lfloor$67, 79$\rfloor$	[358, 422]	[69, 81]
Extracted $\boldsymbol{\lambda}_t >$ estimated $\frac{\theta_\lambda}{\kappa_\lambda}$ and VIX futures in backwardation	**71**	**14**	**69**	**13**
	$\lfloor$42, 94$\rfloor$	$\lfloor$8, 18$\rfloor$	$\lfloor$41, 88$\rfloor$	$\lfloor$8, 17$\rfloor$
Extracted $\boldsymbol{\lambda}_t >$ estimated $\frac{\theta_\lambda}{\kappa_\lambda}$ and VIX futures in contango	**41**	**8**	**35**	**7**
	$\lfloor$19, 104$\rfloor$	$\lfloor$4, 20$\rfloor$	$\lfloor$13, 95$\rfloor$	$\lfloor$3, 18$\rfloor$
Extracted $\boldsymbol{\lambda}_t <$ estimated $\frac{\theta_\lambda}{\kappa_\lambda}$ and VIX futures in backwardation	**13**	**2**	**15**	**3**
	$\lfloor$3, 36$\rfloor$	$\lfloor$1, 7$\rfloor$	$\lfloor$3, 44$\rfloor$	$\lfloor$1, 8$\rfloor$

Panel C: Probability of disasters extracted from weeklys on the S&P 500 index

			Bootstrap CI			Percentiles				
	Mean	SD	Lower	Upper	Min.	P5	P50	P95	Max.	ACF_1
$>$ 8% disaster probability	**0.01206**	0.0234	0.0101	0.0141	0.0006	0.0011	0.0048	0.0491	0.2236	0.79
$>$ 10% disaster probability	**0.00695**	0.0169	0.0056	0.0085	0.0003	0.0006	0.0023	0.0273	0.1836	0.78

Panel D: MLE estimation of the transition density of $\boldsymbol{\lambda}_t$ ($\Delta t = 1/52$)

	8% disaster probability			10% disaster probability		
	κ_λ	$\Delta t \times \frac{\theta_\lambda}{\kappa_\lambda}$	$\sqrt{\Delta t} \times \sigma_\lambda$	κ_λ	$\Delta t \times \frac{\theta_\lambda}{\kappa_\lambda}$	$\sqrt{\Delta t} \times \sigma_\lambda$
Estimate	22.15	0.0121	0.73	26.04	0.0069	0.60
t-stat.	(13.2)	(11.0)	(39.2)	(17.0)	(15.3)	(27.1)

Volatility Uncertainty, Disasters, and the Puzzle of VIX Futures Contango

Internet Appendix: Not Intended for Publication

Abstract

Section A.1 shows that *changes*, over one-month periods, in the slope of the VIX futures curve are predictable by variables *known* at the beginning of the month, such as option implied measures — inferred from equity index options or VIX options — of jump risks and return volatility. Specific drivers of the subsequent variation in the VIX futures curve include (i) jump risks, risk reversals, and butterfly spreads inferred from VIX options, (ii) quadratic variation of the S&P 500 index, and (iii) butterfly spreads inferred from S&P 500 index options.

The purpose of Section A.2 and Section A.3 is to outline, more generally, the sources of risks that impact the slope of the VIX futures curve. We work with a semimartingale model for S_t in combination with Tanaka's formula for semimartingales.

Section A.4 examines the nature of VIX futures contango in a model of equity index dynamics with constant disaster probability and two diffusive volatility components.

A Internet Appendix

A.1 Changes in the slope of the VIX futures curve are predictable

To examine the association between changes in the slope of the VIX futures curve ($\log(\frac{F_t^{(2)}}{F_t^{(1)}})$) and economic variables $\mathrm{q}_t^{[j]}$, we first perform the following univariate predictive regressions with monthly sampled data points:

$$\underbrace{\Delta\text{Slope}^{(2)}_{t+1,\text{vix futures}}}_{\text{change in the slope of the VIX futures curve}} = \theta_0 + \theta_{\mathrm{q}}\,\mathrm{q}_t^{[j]} + \epsilon_{t+1}^{[j]}, \qquad \text{for } j = 1,\ldots,9. \tag{I1}$$

Our inference about θ_{q} is based on the HAC estimator of Newey and West (1987) with automatically selected lags.

Exploring dependencies, we identify nine predictors from S&P 500 and VIX options markets, the construction of which is described in the note to Table I.5. These predictive variables are *known* at time t and can be viewed as encoding information about disaster risks or volatility risks.

Table I.5 (Panel A) imparts the implication that Jump $\text{Risk}_t^{\text{vix}}$, Risk $\text{Reversal}_t^{\text{vix}}$, log VIX_t, Equity $\text{Return}_t^{\text{spx}}$, and Jump $\text{Risk}_t^{\text{spx}}$ exhibit the highest predictive ability. The absolute correlations range between 0.19 and 0.35, with the highest correlation between $\Delta\text{Slope}^{(2)}_{t+1,\text{vix futures}}$ and Jump $\text{Risk}_t^{\text{vix}}$. With a positive θ_{q} estimate, VIX jump risks associates to a stronger subsequent near-term contango. In other words, this effect forecasts the easing of economic concerns.

Since many predictors are informed by options data, one may suspect that some of these variables are cross-correlated. Accounting for this feature, Table I.5 (Panel B) presents bivariate regressions that pairs Jump $\text{Risk}_t^{\text{vix}}$ with other variables, as follows:

$$\Delta\text{Slope}^{(2)}_{t+1,\text{vix futures}} = \theta_0 + \theta_{\{\text{vix jump risk}\}}\,\text{Jump Risk}_t^{\text{vix}} + \theta_{\mathrm{q}}\,\mathrm{q}_t^{[j]} + \epsilon_{t+1}^{[j]}, \quad \text{for } j = 2,\ldots,9. \tag{I2}$$

The variable Jump $\text{Risk}_t^{\text{vix}}$ maintains its significance in the presence of other variables. Overall, this part of our analysis reveals the importance of four other statistically significant predictors: Risk $\text{Reversal}_t^{\text{vix}}$, Butterfly $\text{Spread}_t^{\text{spx}}$, Quadratic $\text{Variation}_t^{\text{spx}}$, and Butterfly $\text{Spread}_t^{\text{vix}}$. The goodness-of-fit $\overline{R}^2$'s in the bivariate regressions range between 11.4% and 14.5%.

Since butterfly spreads are often employed in high volatility environments when investors are apprehensive about near-term equity market outlook, both Butterfly $\text{Spread}_t^{\text{spx}}$ and Butterfly $\text{Spread}_t^{\text{vix}}$ manifest negative predictive coefficients. Thus, these variables tend to forecast a subsequent decline in the near-term slope of the VIX futures curve. In contrast, a more pronounced $\text{Risk Reversal}_t^{\text{vix}}$ or $\text{Quadratic Variation}_t^{\text{spx}}$ aligns with the steepening of the VIX futures curve. In essence, these variables cover data situations that forecast higher near-term volatility uncertainty.

A.2 Sources of risks that impact the slope of the VIX futures curve

Working with a semimartingale model for S_t in conjunction with Tanaka's formula for semimartingales, one can connect $\widetilde{Z}_T$ generically to the price of *local time* (local time can be essentially thought of as a strike dependent variance (as formalized in equation (I11))) and the price of *jumps across the strike* (as formalized in equation (I14)). Our purpose is to motivate a model design.

Formalizing our characterizations, we define the option moneyness $k \equiv \frac{K}{H_T^{T+\hbar}}$. We note that

$$(S_{T+\hbar} - K)^+ \;=\; \max(S_{T+\hbar} - K, 0) \;=\; \max(H_{T+\hbar}^{T+\hbar} - K, 0) \;=\; H_T^{T+\hbar} \max(R_{T+\hbar} - k, 0), \tag{I3}$$

$$\text{where} \qquad R_{T+\hbar} \;=\; \frac{H_{T+\hbar}^{T+\hbar}}{H_T^{T+\hbar}} \;\text{ is the gross futures return between } T \text{ and } T+\hbar. \tag{I4}$$

Analogously, $\max(K - S_{T+\hbar}, 0) = H_T^{T+\hbar} \max(k - R_{T+\hbar}, 0)$. For brevity, we introduce the set

$$\chi_{\text{down}} \equiv \{K < H_T^{T+\hbar}\} = \{k < 1\} \quad \text{and} \quad \chi_{\text{up}} \equiv \{K > H_T^{T+\hbar}\} = \{k > 1\}. \tag{I5}$$

Using Tanaka's formula for semimartingales (as outlined in Internet Appendix (Section A.3)), and spanning $\log(\frac{S_{T+\hbar}}{H_T^{T+\hbar}})$ with the help of option payoffs, it follows that

$$\widetilde{Z}_T \;=\; \mathbb{E}^{\mathbb{Q}}\left(\{ \int_{\chi_{\text{down}}} \frac{2}{\hbar\, K^2} \left(K - H_{T+\hbar}^{T+\hbar}\right)^+ dK + \int_{\chi_{\text{up}}} \frac{2}{\hbar\, K^2} \left(H_{T+\hbar}^{T+\hbar} - K\right)^+ dK \} \Big| \mathcal{I}_T \right) \tag{I6}$$

$$\;=\; \mathbb{E}^{\mathbb{Q}}\left(\{ \int_{\chi_{\text{down}}} \frac{2}{\hbar\, k^2} \left(k - R_{T+\hbar}\right)^+ dk + \int_{\chi_{\text{up}}} \frac{2}{\hbar\, k^2} \left(R_{T+\hbar} - k\right)^+ dk \} \Big| \mathcal{I}_T \right) \tag{I7}$$

$$\;=\; \int_{\chi_{\text{down}}} \frac{2}{\hbar\, k^2}\, \mathbb{E}^{\mathbb{Q}}(L_T[k] \Big| \mathcal{I}_T)\, dk + \int_{\chi_{\text{up}}} \frac{2}{\hbar\, k^2}\, \mathbb{E}^{\mathbb{Q}}(L_T[k] \Big| \mathcal{I}_T)\, dk$$
$$+ \int_{\chi_{\text{down}}} \frac{2}{\hbar\, k^2} \mathbb{E}^{\mathbb{Q}}(J_T^{\text{down}}[k] \Big| \mathcal{I}_T)\, dk + \int_{\chi_{\text{up}}} \frac{2}{\hbar\, k^2} \mathbb{E}^{\mathbb{Q}}(J_T^{\text{up}}[k] \Big| \mathcal{I}_T)\, dk. \tag{I8}$$

In equation (I8), $L_T[k]$ — which represents local time — and $J_T^{\text{down}}[k]$ and $J_T^{\text{up}}[k]$ — which represent jumps across the strike — have a standard representation from Protter (2013), as presented in Internet Appendix (Section A.3).

The takeaway is that $\widetilde{Z}_{T_n}$ encapsulates the uncertainty about the pricing of local time (between T_n and $T_n + \hbar$) and the pricing of jumps across the strike (between T_n and $T_n + \hbar$).

By the Tower law, $\mathbb{E}^{\mathbb{Q}}(\{\tilde{y}\big|\mathcal{I}_T\}\big|\mathcal{I}_t) = \mathbb{E}^{\mathbb{Q}}(\tilde{y}\big|\mathcal{I}_t)$ for a suitable random variable $\tilde{y}$. The interpretation of contango that $F_t^{T_1} < F_t^{T_2}$ for $T_1 < T_2$ (Result 1) accords with the following restrictions:

$$\mathbb{E}^{\mathbb{Q}}(L_{T_1}[k]\big|\mathcal{I}_t) \;\leq\; \mathbb{E}^{\mathbb{Q}}(L_{T_2}[k]\Big|\mathcal{I}_t), \quad \text{for all } k. \tag{I9}$$

$$\mathbb{E}^{\mathbb{Q}}(J_{T_1}^{\text{down}}[k]\big|\mathcal{I}_t) \;\leq\; \mathbb{E}^{\mathbb{Q}}(J_{T_2}^{\text{down}}[k]\big|\mathcal{I}_t) \quad \text{and} \quad \mathbb{E}^{\mathbb{Q}}(J_{T_1}^{\text{up}}[k]\big|\mathcal{I}_t) \;\leq\; \mathbb{E}^{\mathbb{Q}}(J_{T_2}^{\text{up}}[k]\big|\mathcal{I}_t). \tag{I10}$$

If the equity market were to be jittery with elevated jump and volatility risks and no immediate closure were envisioned (e.g., when coronavirus concerns emerged), these restrictions could be violated with an extended pattern of backwardation. The implications of the expressions (I9)–(I10) are made clearer through the models of Section 3.2 and Section 3.3.

A.3 General form of $\widetilde{Z}_T$ in equation (I8) of Section A.2

Set $R_{T+\hbar} \equiv \frac{H_{T+\hbar}^{T+\hbar}}{H_T^{T+\hbar}}$, which is the gross futures return between T and $T + \hbar$. We recognize that $R_T = \frac{H_T^{T+\hbar}}{H_T^{T+\hbar}} = 1$. For the analysis concerning local time and jumps across the strike, we follow Bakshi, Crosby, and Gao (2020).

Recall k is the option moneyness and let $\delta_{\{\bullet\}}$ be the Dirac delta function. We introduce $[R^{\text{c}}, R^{\text{c}}]_\ell$ as the path-by-path continuous part of the quadratic variation, from t to ℓ.

We hereby denote

$$\mathbb{L}_T[k] = \frac{1}{2}\int_T^{T+\hbar} \delta_{\{R_\ell - k\}}\, d[R^{\text{c}}, R^{\text{c}}]_\ell \;\text{ as the } \textit{local time}. \quad \text{(Protter (2013, Theorem 71, page 221))} \tag{I11}$$

The quadratic variation is defined (see Protter (2013, page 70)) as

$$[R^{\text{c}}, R^{\text{c}}]_\ell \;\equiv\; \underbrace{[R, R]_\ell}_{\text{quadratic variation}} \;-\; \underbrace{\sum_{t \leq j \leq \ell} (R_j - R_{j-})^2}_{\text{sum of squares of the return jumps}}. \tag{I12}$$

In our setting, $\mathbb{L}_T[k]$ captures the slice of uncertainty associated with the time that the futures return R_ℓ spends at the level k between T and $T+\hbar$. In economic terms, one may contemplate $\mathbb{L}_t[k]$ as a form of volatility uncertainty when R_ℓ takes a value precisely equal to k.

Additionally, we define

$$J_T^{\text{down}} \equiv \sum_{T<\ell\leq T+\hbar} \mathbb{1}_{\{R_{\ell-}<k\}} \max(R_\ell - k, 0) + \sum_{T<\ell\leq T+\hbar} \mathbb{1}_{\{R_{\ell-}\geq k\}} \max(k - R_\ell, 0), \tag{I13}$$

$$J_T^{\text{up}} \equiv \underbrace{\sum_{T<\ell\leq T+\hbar} \mathbb{1}_{\{R_{\ell-}\leq k\}} \max(R_\ell - k, 0)}_{\text{(jumps crossing the strike from below)}} + \underbrace{\sum_{T<\ell\leq T+\hbar} \mathbb{1}_{\{R_{\ell-}>k\}} \max(k - R_\ell, 0)}_{\text{(jumps crossing the strike from above)}}. \tag{I14}$$

These terms characterize *large deviations* and do not appear in the absence of jumps.

Tanaka's formula for semimartingales. We rely on Tanaka's formula for (general) semimartingales, as in Protter (2013, Theorem 68, page 216):

$$\max(k - R_{T+\hbar}, 0) - \overbrace{\underbrace{\max(k - R_T, 0)}_{=0,\text{ for OTM puts}}}^{\text{intrinsic value}} = - \int_{T+}^{T+\hbar} \mathbb{1}_{\{R_{\ell-}<k\}} dG_\ell + \overbrace{\mathbb{L}_T[k]}^{\text{local time}} + J_T^{\text{down}} \tag{I15}$$

and

$$\max(R_{T+\hbar} - k, 0) - \overbrace{\underbrace{\max(R_T - k, 0)}_{=0,\text{ for OTM calls}}}^{\text{intrinsic value}} = \int_{T+}^{T+\hbar} \mathbb{1}_{\{R_{\ell-}>k\}} dG_\ell + \overbrace{\mathbb{L}_T[k]}^{\text{local time}} + J_T^{\text{up}}. \tag{I16}$$

The term $\int_{T+}^{T+\hbar} \mathbb{1}_{\{R_{\ell-}>k\}}\, dR_\ell$ is a stochastic integral representing the gains/losses to a dynamic trading strategy that takes a long position of size $\frac{1}{H_\ell^{T+\hbar}}$ at time ℓ, in the equity futures, if, and only if, $R_{\ell-} > k$.

Substituting (I15) and (I16) into equation (I7) affirms equation (I8). ■

A.4 Model with constant disaster probability and two diffusive volatility components

For this theoretical exercise, we modify the equity index price dynamics in (14)–(18), following Bates (2000)), in the following way:

$$\text{Size of disasters:} \quad x \qquad \text{follows (unspecified) i.i.d. distribution under } \mathbb{Q} \tag{I17}$$

$$\text{Equity index price :} \quad \frac{dS_t}{S_{t-}} = r\,dt + \sum_{i=1}^{2} \sqrt{\mathbf{v}_t^i}\, d\mathbb{B}_t^{\mathbb{Q},\mathrm{s}^i} + (e^x - 1)\, d\mathbb{N}_t^{\mathbb{Q}} - \boldsymbol{\lambda}\, \mathbb{E}^{\mathbb{Q}}(e^x - 1)dt \tag{I18}$$

$$\text{Poisson jump :} \quad d\mathbb{N}_t^{\mathbb{Q}} = \begin{cases} 1 & \text{with probability } \boldsymbol{\lambda}\, dt \\ 0 & \text{with probability } 1 - \boldsymbol{\lambda}\, dt \end{cases} \tag{I19}$$

$$\text{where } \boldsymbol{\lambda} \text{ is a constant} \tag{I20}$$

$$\text{Two diffusive variances :} \quad d\mathbf{v}_t^i = \left(\theta_{\text{vol}}^i - \kappa_{\text{vol}}^i\, \mathbf{v}_t^i\right) dt \;+\; \sigma_{\text{vol}}^i \sqrt{\mathbf{v}_t^i}\, d\mathbb{B}_t^{\mathbb{Q},\mathbf{v}^i} \qquad \text{for } i = 1, 2. \tag{I21}$$

In this setup, the two volatility components evolve independently and $d\mathbb{N}_t^{\mathbb{Q}}$ uncertainty is uncorrelated with diffusion uncertainty. The standard Brownian motion $\mathbb{B}_t^{\mathbb{Q},\mathrm{s}^i}$ is correlated with $\mathbb{B}_t^{\mathbb{Q},\mathbf{v}^i}$ for each i but otherwise not cross-correlated. Hence,

$$\log(\frac{S_{t+\hbar}}{H_t^{t+\hbar}}) = -\frac{1}{2}\int_t^{t+\hbar} \sum_{i=1}^{2} \mathbf{v}_u^i\, du + \int_t^{t+\hbar} \sum_{i=1}^{2} \sqrt{\mathbf{v}_u^i}\, d\mathbb{B}_u^{\mathbb{Q},\mathrm{s}^i} + \sum_{j=\mathbb{N}_t^{\mathbb{Q}}}^{\mathbb{N}_{t+\hbar}^{\mathbb{Q}}} x_j - \boldsymbol{\lambda}\, \hbar\, \mathbb{E}^{\mathbb{Q}}(e^x - 1). \tag{I22}$$

For a compound Poisson processes with constant intensity, we also have

$$\mathbb{E}^{\mathbb{Q}}\Big(\sum_{j=\mathbb{N}_T^{\mathbb{Q}}}^{\mathbb{N}_{T+\hbar}^{\mathbb{Q}}} x_j \Big| \mathcal{I}_T\Big) = \hbar\, \boldsymbol{\lambda}\, \mathbb{E}^{\mathbb{Q}}(x). \tag{I23}$$

The price of volatility uncertainty over T and $T + \hbar$ is

$$\begin{aligned} \widetilde{Z}_T &= \mathbb{E}^{\mathbb{Q}}(\{-\frac{2}{\hbar}\} \log(\frac{S_{T+\hbar}}{H_T^{T+\hbar}}) \Big| \mathcal{I}_T), \\ &= \mathbb{E}^{\mathbb{Q}}(\{-\frac{2}{\hbar}\}\{-\frac{1}{2} \underbrace{\int_T^{T+\hbar} \sum_{i=1}^{2} \mathbf{v}_u^i\, du}_{\substack{\text{two diffusive volatility risks} \\ \text{over } T \text{ to } T+\hbar}} \} \Big| \mathcal{I}_T) \;+\; \{-\frac{2}{\hbar}\}\{\underbrace{\hbar\, \boldsymbol{\lambda}\, \mathbb{E}^{\mathbb{Q}}(x) - \boldsymbol{\lambda}\, \hbar\, \mathbb{E}^{\mathbb{Q}}(e^x - 1)}_{\substack{\text{time-invariant disaster component} \\ \text{over } T \text{ to } T+\hbar}}\}. \end{aligned} \tag{I24}$$

It holds that

$$\widetilde{Z}_T = \frac{1}{\hbar}\mathbb{E}^{\mathbb{Q}}\left(\int_T^{T+\hbar}\sum_{i=1}^{2}\mathbf{v}_u^i du\Big|\mathcal{I}_T\right) + 2\boldsymbol{\lambda}\mathbb{E}^{\mathbb{Q}}(e^x-1-x) \tag{I25}$$

$$= \sum_{i=1}^{2}\frac{\theta^i_{\text{vol}}}{\kappa^i_{\text{vol}}} + \sum_{i=1}^{2}\frac{(1-e^{-\kappa^i_{\text{vol}}\hbar})}{\hbar\,\kappa^i_{\text{vol}}}\{\mathbf{v}_T^i - \frac{\theta^i_{\text{vol}}}{\kappa^i_{\text{vol}}}\} + 2\boldsymbol{\lambda}\mathbb{E}^{\mathbb{Q}}(e^x-1-x). \tag{I26}$$

In this case, the futures price $F_t^T = \mathbb{E}^{\mathbb{Q}}(\sqrt{\widetilde{Z}_T}\Big|\mathcal{I}_t)$ inherits a two-factor structure in diffusive volatilities.

If $\widetilde{Z}_{T_1}$ is stochastically smaller than $\widetilde{Z}_{T_2}$, that is, $\widetilde{Z}_{T_1} \leq_{\text{st}} \widetilde{Z}_{T_2}$, then, for $T_1 < T_2$,

$$0 \geq \overbrace{\mathbb{E}^{\mathbb{Q}}(\widetilde{Z}_{T_1}|\mathcal{I}_t) - \mathbb{E}^{\mathbb{Q}}(\widetilde{Z}_{T_2}|\mathcal{I}_t)}^{\text{from equation (11) of Result 1}} \quad \text{implying that}$$

$$= \sum_{i=1}^{2}\underbrace{\frac{(1-e^{-\kappa^i_{\text{vol}}\hbar})}{\hbar\,\kappa^i_{\text{vol}}}}_{>0}\underbrace{\{e^{-\kappa^i_{\text{vol}}(T_1-t)} - e^{-\kappa^i_{\text{vol}}(T_2-t)}\}}_{>0}(\mathbf{v}_t^i - \frac{\theta^i_{\text{vol}}}{\kappa^i_{\text{vol}}}). \tag{I27}$$

For $\mathbb{E}^{\mathbb{Q}}(\widetilde{Z}_{T_1}|\mathcal{I}_t) - \mathbb{E}^{\mathbb{Q}}(\widetilde{Z}_{T_2}|\mathcal{I}_t) < 0$, both the volatility factors must be below their respective long-term means. Then, the VIX futures curve supports contango. ■

Table I.1: **Open interest and volume of VIX futures**

Reported entries reflect the daily open interest (contracts outstanding) and volume (number of contracts traded) for VIX futures contracts over the sample period of 04/25/2006 to 12/31/2019.

Displayed are the summary statistics (mean and standard deviation (SD)) for open interest and volume. The starting date coincides with daily futures prices being available for at least six consecutive VIX futures maturities. There are 3,447 daily observations.

Panel A: Daily open interest (number of contracts outstanding)

Contract n	Mean	SD
1	94488	78608
2	81777	71079
3	32000	21287
4	22700	15026
5	17979	12691
6	13135	9824

Panel B: Daily volume (number of contracts traded)

Contract n	Mean	SD
1	58960	61250
2	44616	49519
3	13246	13804
4	6937	6993
5	4155	4222
6	2515	2493

Table I.2: **Futures on the volatility of the STOXX 50 equity index**

For this exercise, we utilize the futures on the VSTOXX index. The VSTOXX index measures the 30-day risk-neutral volatility extracted from options on the EURO STOXX 50 equity index. Reported results are based on daily VSTOXX futures settlement prices over the sample period of 10/22/2010 to 09/23/2021. There are 2,787 daily observations. We compute the slope (in decimal units) as follows:

$$\text{Slope}_t^{(n)} = \log(\frac{F_t^{(n)}}{F_t^{(1)}}), \qquad \text{for } n = 2, \ldots, 6.$$

SD is standard deviation. $\mathbb{1}_{\{\text{Slope}_t^{(n)}>0\}}$ is the fraction (in %) of the observations with positive slopes.

Contango based on six consecutive VSTOXX volatility futures contracts

	Mean	$\mathbb{1}_{\{\text{Slope}_t^{(n)}>0\}}$	SD	Min.	Max.	Percentiles				
						5th	25th	50th	75th	95th
$\log(F_t^{(2)}/F_t^{(1)})$	**0.036**	**74.5**	0.082	-0.396	0.520	-0.094	0.000	0.042	0.077	0.141
$\log(F_t^{(3)}/F_t^{(1)})$	**0.059**	**76.6**	0.108	-0.598	0.510	-0.140	0.006	0.069	0.120	0.213
$\log(F_t^{(4)}/F_t^{(1)})$	**0.070**	**76.7**	0.127	-0.762	0.447	-0.167	0.008	0.080	0.146	0.252
$\log(F_t^{(5)}/F_t^{(1)})$	**0.078**	**76.1**	0.143	-0.856	0.534	-0.170	0.006	0.095	0.165	0.277
$\log(F_t^{(6)}/F_t^{(1)})$	**0.087**	**75.9**	0.154	-0.963	0.509	-0.181	0.007	0.108	0.183	0.306

Table I.3: **Economic states and shape of the VSTOXX futures curve**

The contango feature is depicted across economic states. The economic state is bracketed by daily front-month VSTOXX futures level (Panel A) or daily STOXX 50 index equity returns (Panel B). Reported results are based on daily VSTOXX futures settlement prices over the sample period of 10/22/2010 to 09/23/2021. There are 2,787 daily observations. We compute the slope of the futures curve (in decimal units) as $\text{Slope}_t^{(n)} = \log(\frac{F_t^{(n)}}{F_t^{(1)}})$, for $n = 2, \ldots, 6$. Reported $\mathbb{1}_{\{\text{Slope}_t^{(n)}>0\}}$ is the fraction (in %) of the observations with positive slopes.

Panel A: The market state is front-month VSTOXX futures level

	Lower	< 13	13	15	18	22	30	40	> 50
	Upper		15	18	22	30	40	50	
	Frequency (days)	71	342	567	749	820	175	56	7
	Frequency (%)	2.55	12.27	20.34	26.87	29.42	6.28	2.01	0.25
$\log(\frac{F_t^{(2)}}{F_t^{(1)}})$	Mean	0.151	0.082	0.067	0.042	0.009	-0.035	-0.117	-0.284
	$\mathbb{1}_{\{\text{Slope}_t^{(2)}>0\}}$ (%)	**100**	**97.7**	**88.7**	**81.6**	**60.5**	**33.1**	**3.6**	**0**
$\log(\frac{F_t^{(3)}}{F_t^{(1)}})$	Mean	0.215	0.132	0.102	0.071	0.018	-0.051	-0.191	-0.469
	$\mathbb{1}_{\{\text{Slope}_t^{(3)}>0\}}$ (%)	**100**	**100**	**92.6**	**84.5**	**61.7**	**31.4**	**3.6**	**0**
$\log(\frac{F_t^{(4)}}{F_t^{(1)}})$	Mean	0.274	0.169	0.120	0.085	0.020	-0.075	-0.252	-0.607
	$\mathbb{1}_{\{\text{Slope}_t^{(4)}>0\}}$ (%)	**100**	**100**	**93.8**	**85.8**	**61.6**	**25.7**	**0**	**0**
$\log(\frac{F_t^{(5)}}{F_t^{(1)}})$	Mean	0.306	0.187	0.139	0.095	0.024	-0.085	-0.296	-0.747
	$\mathbb{1}_{\{\text{Slope}_t^{(5)}>0\}}$ (%)	**100**	**100**	**95.6**	**84.9**	**59.8**	**22.9**	**0**	**0**
$\log(\frac{F_t^{(6)}}{F_t^{(1)}})$	Mean	0.322	0.203	0.154	0.109	0.027	-0.095	-0.313	-0.846
	$\mathbb{1}_{\{\text{Slope}_t^{(6)}>0\}}$ (%)	**100**	**100**	**95.9**	**85.8**	**58.4**	**21.1**	**0**	**0**

Panel B: The market state is daily STOXX 50 equity index return

	Return	<-0.035	-0.035	-0.025	-0.015	-0.005	0.005	0.015	0.025	>0.035
	Interval		-0.025	-0.015	-0.005	0.005	0.015	0.025	0.035	
	Frequency (days)	31	53	156	506	1189	614	162	56	20
	Frequency (%)	1.11	1.90	5.60	18.16	42.68	22.00	5.81	2.01	0.72
$\log(\frac{F_t^{(2)}}{F_t^{(1)}})$	Mean	-0.128	-0.016	-0.014	0.028	0.056	0.042	0.019	-0.025	-0.033
	$\mathbb{1}_{\{\text{Slope}_t^{(2)}>0\}}$ (%)	**6.5**	**35.8**	**46.2**	**71.3**	**83.8**	**78.8**	**69.8**	**39.3**	**30.0**
$\log(\frac{F_t^{(3)}}{F_t^{(1)}})$	Mean	-0.204	-0.029	-0.014	0.050	0.087	0.072	0.027	-0.033	-0.055
	$\mathbb{1}_{\{\text{Slope}_t^{(3)}>0\}}$ (%)	**6.5**	**43.4**	**49.4**	**74.3**	**86.0**	**81.2**	**66.0**	**37.5**	**35.0**
$\log(\frac{F_t^{(4)}}{F_t^{(1)}})$	Mean	-0.255	-0.036	-0.017	0.060	0.104	0.086	0.026	-0.048	-0.082
	$\mathbb{1}_{\{\text{Slope}_t^{(4)}>0\}}$ (%)	**6.5**	**39.6**	**48.1**	**75.3**	**86.2**	**81.1**	**66.7**	**39.3**	**30.0**
$\log(\frac{F_t^{(5)}}{F_t^{(1)}})$	Mean	-0.285	-0.041	-0.020	0.067	0.118	0.096	0.029	-0.057	-0.102
	$\mathbb{1}_{\{\text{Slope}_t^{(5)}>0\}}$ (%)	**6.5**	**41.5**	**46.8**	**74.3**	**86.1**	**80.1**	**65.4**	**35.7**	**30.0**
$\log(\frac{F_t^{(6)}}{F_t^{(1)}})$	Mean	-0.311	-0.035	-0.018	0.075	0.130	0.106	0.030	-0.066	-0.109
	$\mathbb{1}_{\{\text{Slope}_t^{(6)}>0\}}$ (%)	**3.2**	**41.5**	**46.2**	**73.7**	**86.2**	**81.3**	**61.7**	**35.7**	**20.0**

Table I.4: **Principal component analysis of the VIX futures prices**

Reported are the principal component coefficients for each of the six VIX futures contracts. Data is daily and the sample period is 04/25/2006 to 12/31/2019 (3,447 daily observations). The last row reports the share of the total variance explained by each of the principal components.

	Principal components					
VIX futures maturity n	PC1	PC2	PC3	PC4	PC5	PC6
1	0.40	0.73	0.52	-0.19	0.06	0.03
2	0.41	0.29	-0.44	0.66	-0.30	-0.17
3	0.41	0.01	-0.50	-0.22	0.64	0.36
4	0.41	-0.19	-0.19	-0.58	-0.28	-0.58
5	0.41	-0.35	0.17	-0.05	-0.51	0.65
6	0.41	-0.47	0.47	0.38	0.40	-0.29
Variance explained (%)	**97.42**	**2.36**	**0.16**	**0.03**	**0.02**	**0.01**

Table I.5: **Variables that forecast the VIX futures curve**

With $\Delta\text{Slope}^{(2)}_{t,\text{vix futures}} = \log(\frac{F^{(2)}_t}{F^{(1)}_t}) - \log(\frac{F^{(2)}_{t-1}}{F^{(1)}_{t-1}})$, the predictive regression is

$$\Delta\text{Slope}^{(2)}_{t+1,\text{vix futures}} \;=\; \theta_{\text{intercept}} \;+\theta_{\text{q}}\, \text{q}^{[j]}_t \;+\; \epsilon^{[j]}_{t+1}, \qquad j = 1, \ldots, 9.$$

Additionally, we examine the bivariate predictive regressions of the type

$$\Delta\text{Slope}^{(2)}_{t+1,\text{vix futures}} \;=\; \theta_{\text{intercept}} \;+\theta_{\{\text{vix jump risk}\}}\, \text{Jump Risk}^{\text{vix}}_t \;+\theta_{\text{q}}\, \text{q}^{[j]}_t + \; \epsilon^{[j]}_{t+1}, \qquad j = 2, \ldots, 9.$$

The variables are constructed in the following manner:

- Jump $\text{Risk}^{\text{vix}}_t$: Price of a 20% OTM VIX put divided by the VIX futures price.
- Risk $\text{Reversal}^{\text{vix}}_t$: Implied volatility of a 20% OTM VIX put divided by the implied volatility of the 20% OTM VIX call.
- Logarithm VIX_t: Logarithm of the VIX index.
- Equity $\text{Return}^{\text{spx}}_t$: Prior return of the S&P 500 equity index.
- Jump $\text{Risk}^{\text{spx}}_t$: Price of a 5% OTM S&P 500 put divided by the level of the S&P 500 index (e.g., Bollerslev and Todorov (2011)).
- Butterfly $\text{Spread}^{\text{spx}}_t$: Implied volatility (average) of a 5% OTM put and call divided by the average implied volatility of an ATM put and call.
- Quadratic $\text{Variation}^{\text{spx}}_t$: Squared (log) S&P 500 returns, summed over the *prior* expiration cycle.
- Change in ATM Implied $\text{Volatility}^{\text{vix}}_t$: Reflects the change in the implied volatility (average) of an ATM VIX put and call over the *prior* expiration cycle.
- Butterfly $\text{Spread}^{\text{vix}}_t$: Implied volatility (average) of a 20% OTM VIX put and call divided by the average implied volatility of an ATM VIX put and call.

The data is sampled monthly and contains 163 observations. The intercept is included in the regressions but not reported. For ease of comparability, each predictor is standardized to have zero sample mean and unit standard deviation. Reported NW[p] is based on the HAC estimator of Newey and West (1987) with automatically selected lags, and Corr (in Panel A) is the correlation between $\Delta\text{Slope}^{(2)}_{t+1,\text{vix futures}}$ and the predictor. $\overline{R}^2$ is the adjusted R^2 and DW is the Durbin Watson statistic.

Panel A: Univariate regressions

	Univariate predictor	Predictor θ_{q} $\times 10^{-2}$	Predictor NW[p]	$\overline{R}^2$	Corr	NW lag	DW
1	Jump $\text{Risk}^{\text{vix}}_t$	1.77	0.00	12	0.35	4	2.5
2	Risk $\text{Reversal}^{\text{vix}}_t$	1.60	0.00	9	0.32	6	2.5
3	Logarithm VIX_t	1.48	0.00	8	0.29	4	2.5
4	Equity $\text{Return}^{\text{spx}}_t$	-1.34	0.00	6	-0.26	1	2.4
5	Jump $\text{Risk}^{\text{spx}}_t$	1.33	0.00	6	0.26	5	2.6
6	Butterfly $\text{Spread}^{\text{spx}}_t$	-1.14	0.00	4	-0.23	7	2.6
7	Quadratic $\text{Variation}^{\text{spx}}_t$	1.10	0.00	4	0.22	5	2.6
8	Change in Implied $\text{Volatility}^{\text{vix}}_t$	1.05	0.02	4	0.21	4	2.4
9	Butterfly $\text{Spread}^{\text{vix}}_t$	-0.98	0.00	3	-0.19	4	2.5

Panel B: Bivariate regressions

		Jump $\text{Risk}^{\text{vix}}_t$		Other predictor		$\overline{R}^2$	DW
	Other predictor ($\text{q}^{[j]}_t$)	$\theta_{\{\text{vix jump risk}\}}$ $\times 10^{-2}$	NW[p]	θ_{q} $\times 10^{-2}$	NW[p]		
Jump $\text{Risk}^{\text{vix}}_t$	Risk $\text{Reversal}^{\text{vix}}_t$	1.27	0.01	0.76	0.10	12.4	2.5
Jump $\text{Risk}^{\text{vix}}_t$	Logarithm VIX_t	1.39	0.01	0.61	0.15	12.0	2.5
Jump $\text{Risk}^{\text{vix}}_t$	Equity $\text{Return}^{\text{spx}}_t$	1.49	0.00	-0.52	0.24	11.8	2.4
Jump $\text{Risk}^{\text{vix}}_t$	Jump $\text{Risk}^{\text{spx}}_t$	1.50	0.00	0.50	0.06	11.8	2.5
Jump $\text{Risk}^{\text{vix}}_t$	Butterfly $\text{Spread}^{\text{spx}}_t$	1.56	0.00	−0.56	0.03	12.2	2.5
Jump $\text{Risk}^{\text{vix}}_t$	Quadratic $\text{Variation}^{\text{spx}}_t$	1.59	0.00	0.46	0.01	11.8	2.5
Jump $\text{Risk}^{\text{vix}}_t$	Change in Implied $\text{Volatility}^{\text{vix}}_t$	1.63	0.00	0.33	0.53	11.4	2.4
Jump $\text{Risk}^{\text{vix}}_t$	Butterfly $\text{Spread}^{\text{vix}}_t$	1.74	0.00	−0.93	0.00	14.5	2.4

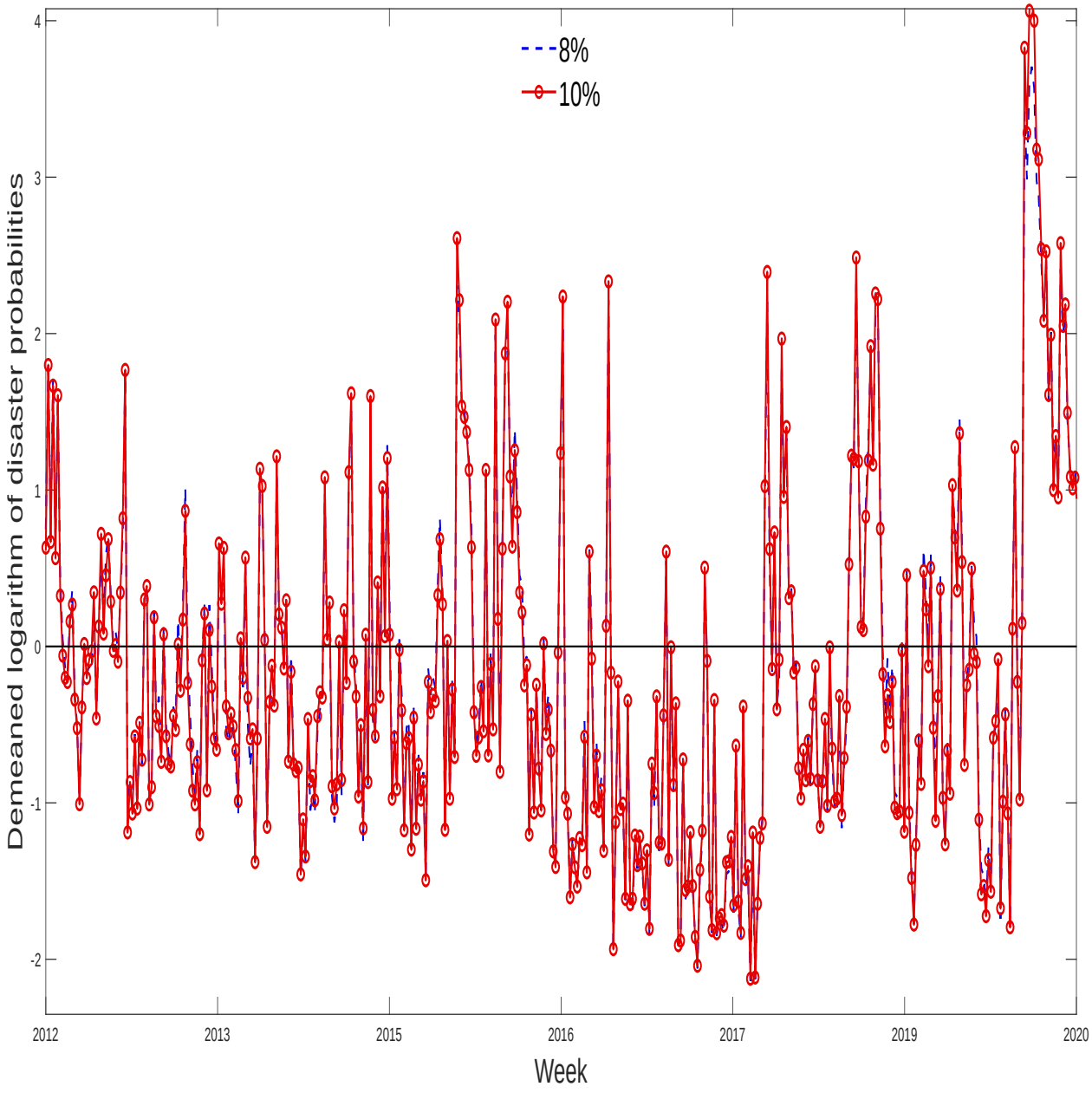

Figure I.1: **Variations in demeaned logarithm of disaster probabilities**

Plotted is the demeaned $\log(\boldsymbol{\lambda}_t)$ for visual convenience. We employ equation (29) to extract the risk-neutral disaster probability over 519 weeks in our sample of weekly put options on the S&P 500 equity index from 1/7/2011 to 12/18/2020. These weeklys on the S&P 500 equity index maintain a fixed option maturity of 7 days (Friday to Friday).